Construction and Building Materials 322 (2022) 126338

Contents lists available at ScienceDirect

Construction and Building Materials

journal homepage: www.elsevier.com/locate/conbuildmat

Rheological, fresh, and mechanical properties of mechanochemically activated geopolymer grout: A comparative study with conventionally activated geopolymer grout

Mukhtar Hamid Abed [a,b], Israa Sabbar Abbas [a], Majid Hamed [c], Hanifi Canakci [d,*]

[a] Department of Civil Engineering, Gaziantep University, Gaziantep, Turkey
[b] Department of Civil Engineering, University of Anbar, Anbar, Iraq
[c] Department of Civil Engineering, Kirkuk University, Kirkuk, Iraq
[d] Department of Civil Engineering, Hasan Kalyoncu University, Gaziantep, Turkey

ARTICLE INFO

Keywords:
Grouting
Mechanochemical activation
Geopolymer
Rheological
Setting time
Strength
Slag
Fly ash

ABSTRACT

In this research, a mechanochemically activated geopolymer (MG) grout is adopted to activate slag, fly ash, sodium hydroxide, and sodium silicate by dry grinding in a ball mill for 2 h, after which water is the only additive required to initiate the geopolymerization reaction. A conventionally activated geopolymer (CG) grout was also evaluated for comparison purposes. Twenty-four different slag and fly ash mixtures have been prepared at different slag/fly ash ratios (0S100F, 50S50F, 75S25F, and 100S0F) at three different molarities of sodium hydroxide (1.25, 2.5, and 3.75) to assess the behavior of both MG grout and CG grout. A series of tests were examined, such as rheological characteristics, setting time, bleeding, unconfined compressive strength (UCS), ultrasonic pulse velocity (UPV), and scanning electron microscopy (SEM). The experimental results showed that the mechanochemical activation technique reduced the rheological characteristics and fresh properties (setting time and bleeding) of geopolymer grout compared to the conventional activation process. Considering mechanical properties, both UCS and UPV of MG grout were higher than that of CG grout. Furthermore, slag content and sodium hydroxide concentration significantly affected the rheological, fresh, and mechanical properties of all geopolymer grouts regardless of the activation method. Both the rheological characteristics and mechanical properties were increased considerably with the increase in molar concentration and slag content. Whereas the bleeding capacity and setting time dramatically reduced with the increase of molar concentration and slag content.

1. Introduction

Grouting is one of the effective methods for ground improvement in the construction sector (e.g., tunnels, anchors, dam barriers, pre-stressed coating cables, building foundations, etc.) [1-3]. The construction industry is considered a higher consumer of Portland cement, and many grouting applications rely on cement for ground improvement in conventional practice. However, the previous studies stated that the over-dependence on Portland cement has led to ecological issues such as large CO_2 emissions, resource depletion, dust generation, etc. [4-6]. Furthermore, the utilization of Portland cement has been found to have side effects like high bleeding, high plastic shrinkage, and some strength problems owing to the loss of water and incomplete hydration at early ages [7,8]. To eliminate these issues, many researchers paid considerable attention to replacing cement with pozzolanic materials or some admixtures by considering better grout performance with some eco-friendly materials [9-12]. In the last two decades, a new type of material called geopolymer has been successfully adapted in construction works, and it could be a good alternative material for grouting applications instead of cement [13-15].

The geopolymer binder consists of alumina-silica sources such as metakaolin, slag, rice husk ash, and fly ash activated with an alkali activator solution like sodium or potassium hydroxide and sodium silicate [4,5,7,16]. Geopolymer materials are environmentally friendly, durable, highly resistant to chemical attack, resistant to alkali-aggregate reaction, possessing good mechanical performance, and viscoplastic behavior similar to conventional cement, etc. [6,17-24]. Despite the remarkable greenness potential of geopolymer, which promotes its

* Corresponding author.
E-mail addresses: majid79@uokirkuk.edu.iq (M. Hamed), hanifi.canakci@hku.edu.tr (H. Canakci).

https://doi.org/10.1016/j.conbuildmat.2022.126338
Received 11 October 2021; Received in revised form 12 December 2021; Accepted 3 January 2022
Available online 18 January 2022

Table 1
chemical and physical properties of FA, slag, and sodium silicates.

Constituent (%)	Slag	Fly ash	(Na_2SiO_3-Penta) Powder	(Na_2SiO_3) liquid
a) Chemical composition				
Cao	34.19	4.24		
SiO_2	40.42	57.2	28	29.4
$Al2O_3$	10.6	24.4		
Fe_2O_3	1.28	7.1		
MgO	7.63	2.4		
SO_3	0.68	0.29		
K_2O	0.0128	3.37		
Na_2O		0.38	29	14.7
Modulus ratio			1	2
H_2O			43[a]	55.9
b) Physical properties				
Specific surface (m^2/kg)	565	379		
Specific gravity	2.9	2.2		

[a]Chemically bound water in the powder which is released when dissolved in water.

application as a promising alternative binder to Portland cement; however, the use of geopolymer has been restricted to small-scale applications. To make the most of the excellent eco-friendly geopolymer, large-scale applications of geopolymer in the construction industry should be really taken into consideration. Conventionally, geopolymer is manufactured from a two-part mix comprising solid aluminosilicate precursors and alkaline solutions. These user-hostile activator solutions are frequently used to dissolve the aluminosilicate source materials and govern the mechanical properties of the geopolymer binder, such as its compressive strength [25,26]. There are several pitfalls regarding the two-part mix formulations used in the synthesis of "traditional" geopolymers [27]. Handling large quantities of highly corrosive and often viscous alkaline solutions would be difficult to use for commercial and mass production of geopolymer materials and hinders the large-scale application of geopolymer. In addition, the rheology of the geopolymer can be difficult and complex to control as a result of the formation of a thick paste and sticky, particularly in geopolymer systems where sodium is the source of alkali [28]. Moreover, the geopolymer system is sensitive to the ratio of alkali to available silicate, which can be challenging to control in practice where waste materials are used as a silica source [29]. Lastly, as a result of the movement of alkalis and water to the geopolymer surface during curing or in service, there can be a tendency toward efflorescence, and/or high permeability and water absorption, unless the water and alkali content of a geopolymer mix are cautiously controlled [4,30]. Thus, one of the main steps towards the large-scale application of geopolymer in the construction industry is developing a one-part "just add water" geopolymer mixture as an alternative method that is more similar to the utilization of conventional Portland cement-based materials.

One-part geopolymers are made with blends of solid alkaline activators and solid aluminosilicates precursors [31-33]. The use of solid activators in the manufacture of geopolymer enhances its commercial viability because it aids the development of a one-part "just add water" mixture, similar to conventional cement-based materials [34]. Only recently, some studies focused on synthesizing one-part geopolymer. For instance, Koloušek et al. [35] developed a one-part geopolymer mix by making a totally sodium silicate-free geopolymer system by calcination of kaolinite or halloysite together with powdered hydroxides, but this was reported to result in low strength development (7-days strengths<1 MPa were given). Suwan et al. [36] obtained binder samples by ambient temperature curing with a strength of 2.4 and 6.0 MPa after 7 and 28 days of curing, respectively. Nematollahi et al. [34] prepared one-part geopolymer mortar specimen by 60 °C curing, obtaining a compressive strength of 29.3 MPa after 7 days. Askarian et al. [37] reports that mortar specimen activated with sodium silicate cured at 60 °C showed a compressive strength of 12.3 MPa after seven days; the same mix design cured at ambient temperature exhibited a compressive strength of 7.0 and 10.9 MPa after 7 and 28 days, respectively; and they also reported that ambient temperature-cured one-part geopolymer obtained by mixing fly ash and Na-based solid activator was not able to set in 24 h and did not exhibit any strength even after 3 days.

From the previous studies, only low mechanical performances have been achieved when room-temperature curing was applied. In addition, one-part geopolymers are mainly studied considering heat curing, thus limiting the potential application fields of these systems where heating is not allowed (e.g., grouting, building materials for in situ applications, materials for rendering, restoration, etc.) [31]. Thus, in this study, mechanochemical treatment was employed to improve the reactivity of a one-part geopolymer during ambient curing and as a substitute activation strategy for overcoming the challenges associated with conventional two-part geopolymers. A mechanochemical activation is an approach for making geopolymers via an innovative solid-state chemistry mechanism. It requires binders in solid form such as alumina-silica source and solid alkaline activators blended in a ball mill, and therefore, only water has to be added to initiate the geopolymerization process [38]. Mechanochemical activation is a process of co-grinding or co-milling small particulate solid matter to perform molecular dense, reactive, and amorphous aggregated composite particles. The intense grinding and milling process can form electrostatic charges and defects on the surface particles, increasing the surface energy and generating crystalline changes to the amorphous phase [39,40] and activated particle agglomeration [41]. On the other hand, mechanically activating powder (slag or fly ash) can increase the reactivity, causes damage and breakdown of crystalline structure, and alter polymerized unit structure [42]. Mucsi et al. [43] made a comparison between small and large-sized particles of mechanically activating fly ash powder. The results showed that the small-sized particles exhibited different polymerized unit structures than larger particles. The results also showed influences reaction rate, particle dissolution, geopolymerization reaction, mechanical strength, and increases in water demand of mechanically activating powder [44-46]. Mechanochemical activation of alkaline activator with fly ash for an extended period has also been demonstrated, and greatly enhanced the mechanical performance of geopolymer systems and enhances heavy metal stabilization [47-51].

Analysis of the previously published works showed that the rheological, fresh, and mechanical properties of mechanochemically activated geopolymer grout were not introduced in the published literature, therefore, this study aims to fill the research gap and gain an in-depth understanding of the behavior of MG grout in comparison with CG grout. In the current research, a mechanochemical process is adopted for activating slag, fly ash, sodium hydroxide, and sodium silicate by dry grinding in a ball mill for 2 h. Just water is added to the geopolymeric precursor (MG powder). In addition to the activation method, the effect of slag to fly ash ratio and the molarity of sodium hydroxide were also assessed. A series of tests were examined to evaluate the behavior of both MG and CG grouts through yield stress, plastic viscosity, setting time, bleeding, density, ultrasonic pulse velocity, unconfined compressive strength, and scanning electron microscopy.

2. Experimental program

2.1. Materials

low calcium fly ash (class F) was used in this study to produce both CG and MG. The disposal of coal fly ash powder in landfills diminishes the valuable fertile land. Therefore, its disposal and utilization in an appropriate way are essential. Fly ash-based geopolymer grout has high workability, good durability against aggressive environments, and low shrinkage [52-54]. However, the limiting factor for wider use of fly ash for geopolymer synthesis owing to its low reactivity and low strength gain when cured at room temperature [55-57]. To tackle the low

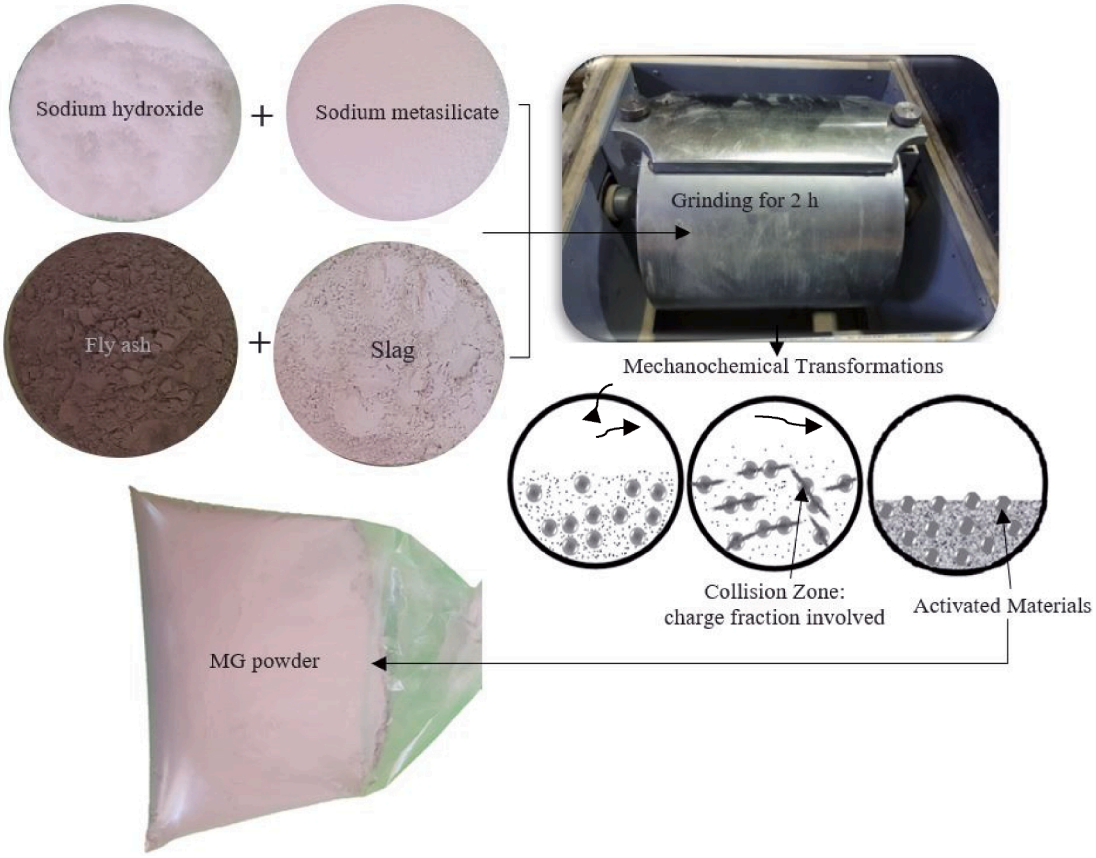

Fig. 1. The production process of MG powder.

Table 2
Mix proportions of CG and MG-based grout.

		Weight: %					Weight: (g)				
Molarity	Mix ID	Fly ash %	Slag %	NaOH %	Na_2SiO_3 %	Grindingduration:h	Fly ash (g)	Slag (g)	NaOH (g)	Na_2SiO_3 (g)	Water (g)
1.25	CG-0S100F	85	0	10	5[a]	–	850	0	100	50	1250
	CG-50S50F	42.5	42.5	10	5[a]	–	425	425	100	50	1250
	CG-75S25F	21.25	63.75	10	5[a]	–	212.5	637.5	100	50	1250
	CG-100S0F	0	85	10	5[a]	–	0	850	100	50	1250
	MG-0S100F	85	0	10	5[b]	2	850	0	100	50	1250
	MG-50S50F	42.5	42.5	10	5[b]	2	425	425	100	50	1250
	MG-75S25F	21.25	63.75	10	5[b]	2	212.5	637.5	100	50	1250
	MG-100S0F	0	85	10	5[b]	2	0	850	100	50	1250
2.5	CG-0S100F	85	0	10	5[a]	–	850	0	100	50	1000
	CG-50S50F	42.5	42.5	10	5[a]	–	425	425	100	50	1000
	CG-75S25F	21.25	63.75	10	5[a]	–	212.5	637.5	100	50	1000
	CG-100S0F	0	85	10	5[a]	–	0	850	100	50	1000
	MG-0S100F	85	0	10	5[b]	2	850	0	100	50	1000
	MG-50S50F	42.5	42.5	10	5[b]	2	425	425	100	50	1000
	MG75S25F	21.25	63.75	10	5[b]	2	212.5	637.5	100	50	1000
	MG-100S0F	0	85	10	5[b]	2	0	850	100	50	1000
3.75	CG-0S100F	85	0	10	5[a]	–	850	0	100	50	750
	CG-50S50F	42.5	42.5	10	5[a]	–	425	425	100	50	750
	CG-75S25F	21.25	63.75	10	5[a]	–	212.5	637.5	100	50	750
	CG-100S0F	0	85	10	5[a]	–	0	850	100	50	750
	MG-0S100F	85	0	10	5[b]	2	850	0	100	50	750
	MG-50S50F	42.5	42.5	10	5[b]	2	425	425	100	50	750
	MG-75S25F	21.25	63.75	10	5[b]	2	212.5	637.5	100	50	750
	MG-100S0F	0	85	10	5[b]	2	0	850	100	50	750

[a] Composed of the sodium silicate Na_2SiO_3″ activator (in liquid form).
[b] Composed of sodium metasilicate (SMS; Na_2SiO_3) -Penta" activator (in powder form).

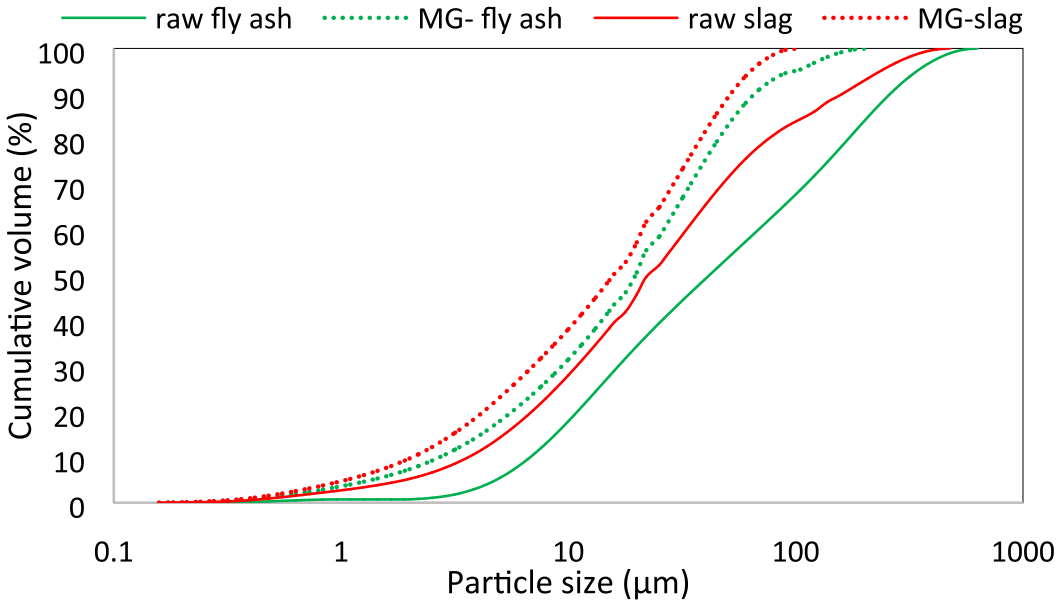

Fig. 2. Particle size distribution of the raw and mechanochemical grinding slag and fly ash.

reactivity of used fly ash in this study, slag is incorporated in the fly ash-based geopolymer grout because it possesses high mechanical strength and good durability in corrosive environments [58]. However, slag binder has some problematical properties such as poor workability, high viscosity, fast setting, and high shrinkage [59-63]. The previously published works showed that the combination of both slag and fly ash in synthesis geopolymer grout shows higher reactivity, better compressive strength, and lower shrinkage as compared to the full slag or fly ash-based geopolymer grout [57,64-66].

Sodium silicate and NaOH were chosen in this study as the alkaline activator. Sodium hydroxide solution was prepared one day before mixing with different molar concentrations (1.25, 2.5, and 3.75 M) using NaOH beads of 97–98% purity locally purchased and dissolved in faucet water. Sodium silicate (Na_2SiO_3) was used in two forms, a powder form (metasilicate-Penta) for preparing mechanochemical geopolymer and a liquid solution for preparing the conventional geopolymer. Based on previously published works that adopted the mechanochemical activation approach, a ratio of Na_2SiO_3/NaOH = 0.5 was selected to prepare the alkaline activator [49,67-70]. Table 1 displays the chemical and physical properties of the precursor components (FA and slag) and sodium silicate in both liquid and powder forms.

2.2. Geopolymer preparation

Geopolymerization is a process that produces cementitious composites using alkaline activation and aluminosilicate-rich materials. In this research, MG, in addition to the CG, has been adopted for preparing geopolymer grout. Regarding CG preparations, sodium hydroxide beads were calculated and weighed based on the desired molarity (1.25, 2.5, and 3.75 M) and dissolved in tap water. An exothermic reaction occurred during the mixing time, and the liquid became very hot. For that reason, the liquid was stored at ambient temperature before it was used till the chemical equilibrium was gained then, after the NaOH solution being cooled down, the sodium silicate was added. In general, the alkali activator liquid was prepared at least one day before mixing the CG ingredients.

For MG grout, all raw materials powder (NaOH, metasilicate, slag, and fly ash) were grinded for 2 h using a ball mill of 80 kg capacity using 12 balls, each with a mass of 400 g and diameter of 45 mm. Through the ball milling process (grinding), the components (particles) of mixed raw materials are trapped between the balls and the container wall that was caused the continuous impact of the particles and grinding. After that, the obtained MG powder was mixed with faucet water to manufacture MG grout, as shown in Fig. 1.

Two mixture groups (MG and CG) were used in this study, and each group contains four different mix proportions (0% slag – 100% fly ash, 50% slag – 50% fly ash, 75% slag – 25% fly ash, and 100% slag – 0% fly ash). For example, the MG-100S0F code means that the grout type mechanochemically activated geopolymer grout with 100% slag and zero fly ash. Also, the CG-75S25F code signifies that the adopted grout is conventionally activated geopolymer included 75% slag and 25% fly ash. On the other hand, the influence of the molar concentration of sodium hydroxide has also been taken into consideration. Therefore, three different concentrations (1.25, 2.5, and 3.75 M) were used in this investigation to reveal the effect of molarity on the rheological fresh and mechanical properties of both MG and CG grout. Table 2 presents all the mixture proportions of both CG and MG grouts.

2.3. Testing methods

All the prepared specimens were produced in the laboratory at room temperature 23 ± 3 °C. To examine the rheological properties, the rheological tests were carried out based on the ASTM D4016-08 [71] using a rational viscometer (proRheo R 180). A coaxial cylinder was used, the shear stress was obtained at different shear rates 500 s^{-1}, 571.43 s^{-1}, 642.86 s^{-1}, 714.29 s^{-1}, 785.71 s^{-1}, 857.14 s^{-1}, 928.57 s^{-1}, and 1000 s^{-1} [8,72,73]. According to preliminary trials, all the shear rate was kept constant duration time of 15 s to obtain an equilibrium state in a total of 2 min for completing the test of each mixture.

The apparent viscosity and the shear stress versus the shear rate represented by the flow curves have been determined for both portions (ascending and descending) though only the results obtained by the ascending portion were taken into account in this study [74-77]. In nonlinear responses for the rheological curves, the dilatant (shear-thickening) performance occurs when both shear rate and viscosity increase. Nevertheless, in a negative gradient, the viscosity decreases with increasing shear rate, the flow leads to the pseudoplastic (shear-thinning) performance [75]. The yield stress is related to cohesion in soil or slump in concrete corresponds to the least shear stress to create the flow grout, while the plastic viscosity can be related to stickiness, pumpability, finishability, placeability, and segregation [76,78]. In this study, a modified Bingham model has been adopted by the previous studies

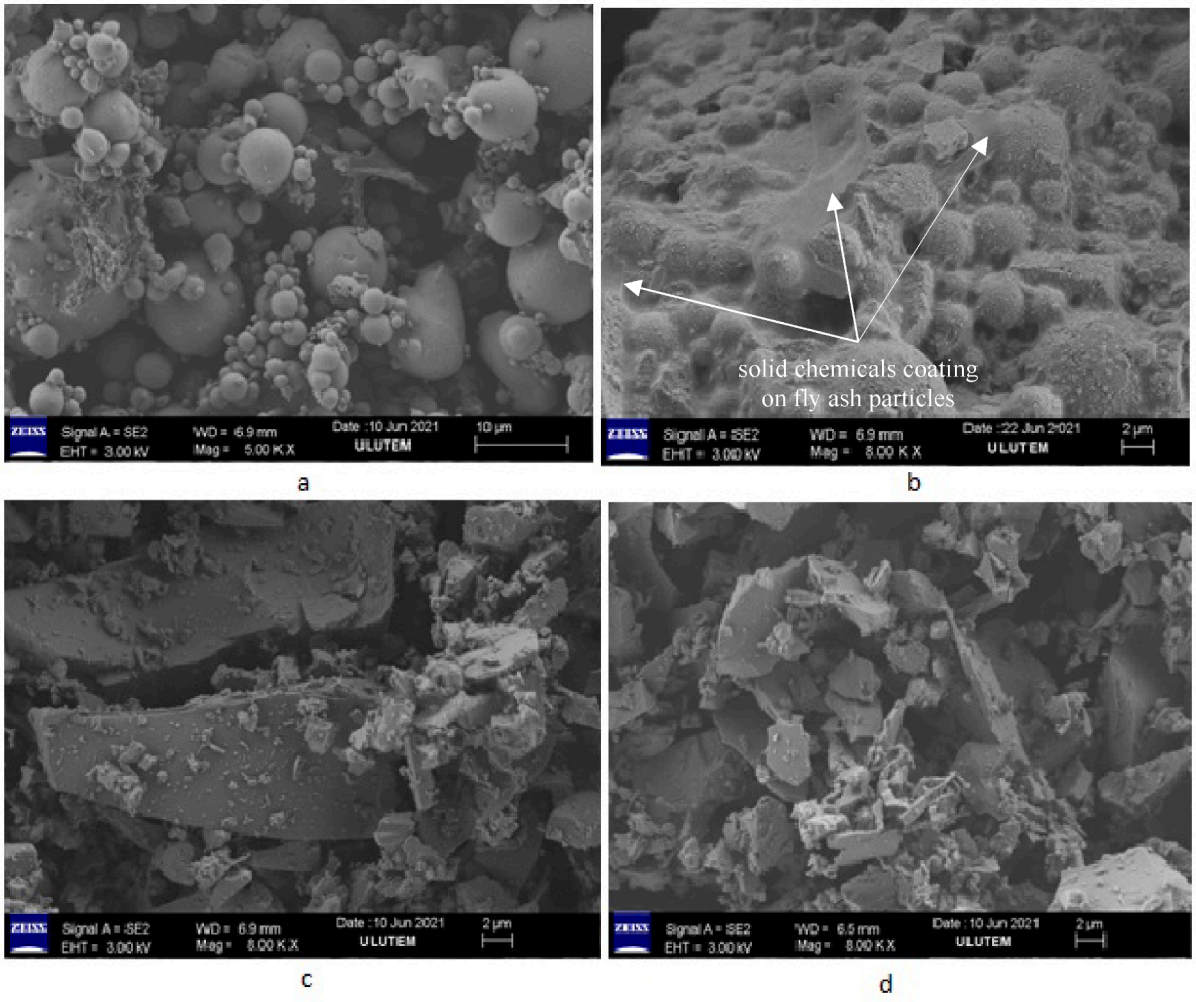

Fig. 3. SEM images of (a) raw fly ash, (b) MG fly ash, (c) raw slag, and (d) MG slag.

[74,75,78], and the plastic viscosity and yield stress were obtained as following Eq (1):

$$\tau = \tau_0 + \mu_p \dot{\gamma} + c\dot{\gamma}^2 \quad (1)$$

where, τ_0 is the yield stress (Pa), τ is stress (Pa),$\dot{\gamma}$ is the shear rate (s^{-1}), μ_p is the plastic viscosity (Pa.s), and C is a constant. The coefficient (C) can be applied to describe non-linear behavior, indicating shear thinning ($C < 0$), shear thickening ($C > 0$) and the Bingham model ($C = 0$) [79-81]. Vicat needle test was adopted to measure the initial and final setting time as recommended by ASTM C191-19 [82]. The initial setting time can be defined as the time passed between the instants when the water is supplemented to the cement to the time when the square needle of the Vicat device penetrates a depth of 25 mm from the top. The same expression can be applied to define the final setting time; the latter can be defined as the time passed between the instants when the water is supplemented to the cement and when the cement paste has fully missed its plasticity. An important point must be taken into account. The bleeding capacity is calculated by ASTM C940-16 [83]. A graduated cylinder with 1000 mL was used for the grout mixture; the poured mixture inside the cylinder was left for two hours for completing the sedimentation of the mixture suspension. It is reported that the grout is stable when the bleeding capacity is $< 5\%$ or 10% after two hours of mixing [84].

Regarding mechanical properties, the grout mixtures were poured in cylindrical molds; the height and diameter of cylindrical molds are 100 mm and 50 mm, respectively. The samples were cured at a temperature of 23 ± 3 °C till the testing date (7 and 28 days). Then, the unconfined compressive strength (UCS) of grout samples was tested by standards [85,86]. It is important to mention that, before conduction the UCS testing, the samples were used to measure the wave velocity (UPV) by ASTM C597–09 [87]. The UPV, defined as a non-destructive test, was used to examine the stiffens of hardened samples. Previous studies revealed that there are many different classes of quality to indicate the hardened of the sample (very low velocity UPV < 2500 m/s; low velocity UPV 2500–3500 m/s; middle velocity 3500–4000 m/s; high velocity UPV 4000–5000 m/s; and very high velocity UPV > 5000 m/s) [8,88].

3. Results and discussion

3.1. Analysis of microstructure

The grain size is considered to have the main role in the variation of mechanical and rheological properties. The particle size distribution curves of slag and fly ash for raw and mechanochemical grinding were presented in Fig. 2. D50 (median size) of raw slag and fly ash were 22 μm, and 38 μm while the median size of slag and fly ash (after blending with sodium silicate and NaOH in ball milling for 2 h) was decreased to 15 μm and 20 μm respectively, as seen in Fig. 2.

Scanning electron microscopy (SEM) analysis illustrated the microstructure approach of raw and mechanochemical grinding slag and fly ash precursors. In Fig. 3a, it can be detected that the majority of the raw fly ash particles were mostly spherical shape. After grinding fly ash with

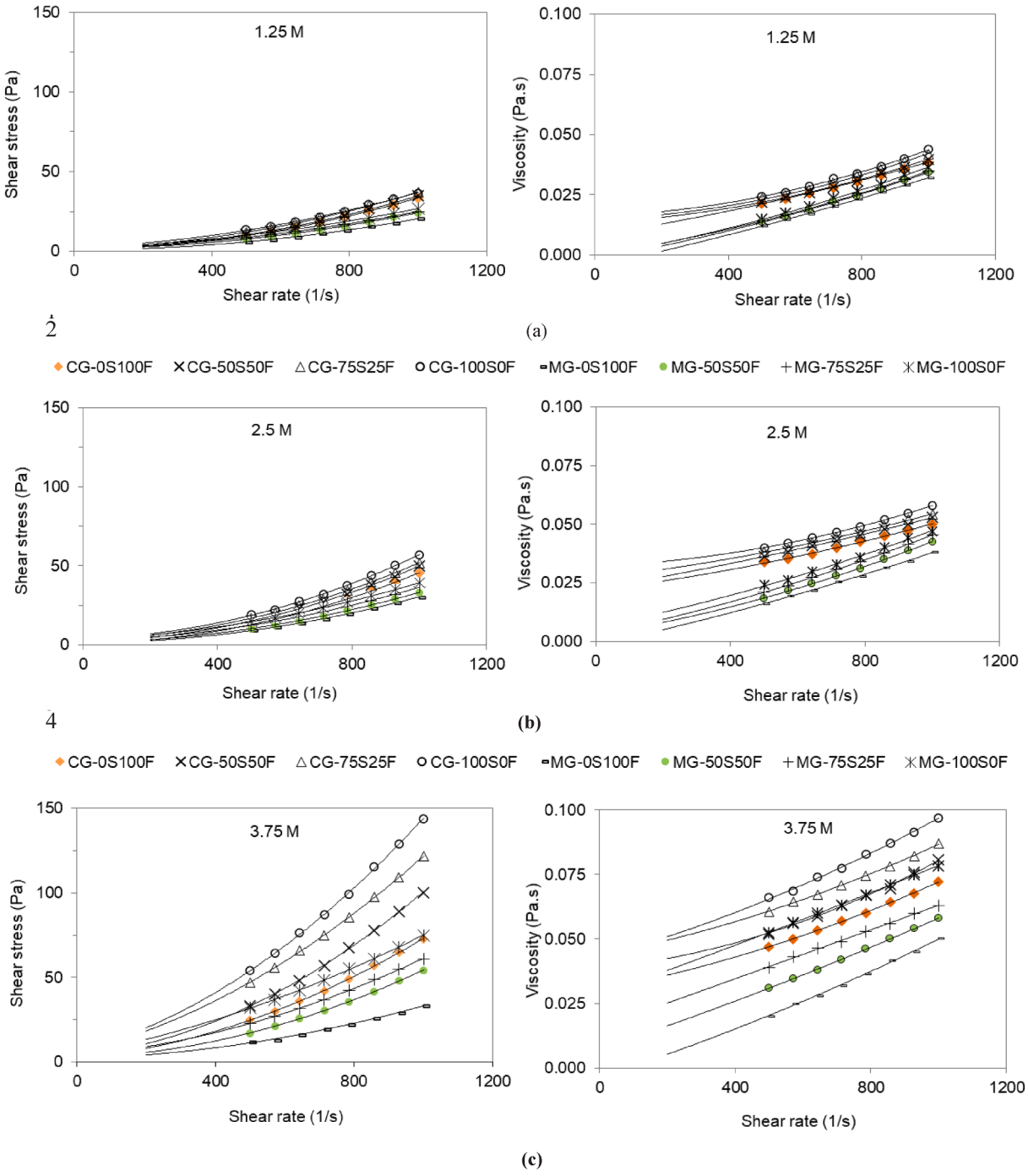

Fig. 4. The rheological curves of CG and MG-based grout, (a) 1.25 M; (b) 2.5 M; (c) 3.75 M.

sodium metasilicate and sodium hydroxide, the fly ash particles have been coated by solid chemical powder (the combination of sodium silicate and hydroxide), which caused a reduction in the solid chemicals and average size of fly ash. However, the spherical morphology of the raw fly ash was not fully destroyed, and there was some agglomeration of the fine-grained particles. Thus, the formation of the geopolymeric precursor has been produced. In addition, the initial binding was observed between fly ash particles because of the addition of sodium hydroxide and metasilicate. Moreover, Gupta et al. [38] reported that the ball-milling of sodium hydroxide and fly ash together for 8 h led to the development of cracks and defects, resulting in an increase in surface area and enhanced reaction. SEM analysis of raw slag and MG slag precursor was also reported in this study. Fig. 3c, d showed the SEM images of raw slag and MG slag precursor at a magnification of 8000 times. As seen in Fig. 3c, the size and shape of slag particles were dissimilar and heterogeneous, and the material components appear as subrounded to angular shapes. The edges and roughness were observable in angular particles and bulk [89]. After the mechanochemical process of slag, it's evident that the size of slag particles was generally reduced (Fig. 3d), and it still has angular and deforms shapes. Also, the mechanochemical process for 2 h increased the surface area of the particles and imparted a higher reaction rate of the geopolymer precursors.

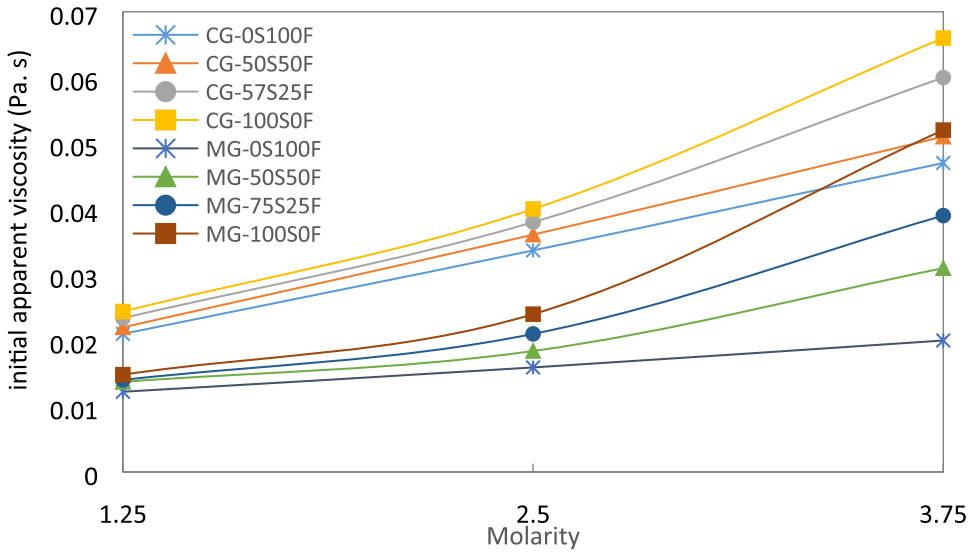

Fig. 5. Variations of the initial apparent viscosity of CG and MG-based grout at different Molarity.

Table 3
Rheological characteristics of CG and MG-based grout.

Molarity	Mix ID	initial apparent viscosity (Pa. s)	coefficient C	τ_0 (Pa)	μ_p (Pa. s)	Grout Temperature [°C]
1.25	CG-0S100F	0.021	0.00003	1.37	0.0044	22.4
	CG-50S50F	0.022	0.00003	1.64	0.0059	22.7
	CG-57S25F	0.0234	0.00003	1.738	0.00852	23
	CG-100S0F	0.0244	0.00003	2.22	0.019	23
	MG-0S100F	0.0122	0.00002	0.701	0.0029	28.2
	MG-50S50F	0.0137	0.00002	1.49	0.0038	28.5
	MG-75S25F	0.014	0.00002	1.61	0.0069	29
	MG-100S0F	0.0148	0.00002	1.87	0.00874	29
2.5	CG-0S100F	0.0337	0.00004	1.65	0.0061	23
	CG-50S50F	0.0361	0.00004	1.96	0.0093	23
	CG-57S25F	0.0380	0.00004	3.04	0.016	23
	CG-100S0F	0.0400	0.00005	3.762	0.0362	23
	MG-0S100F	0.0159	0.00003	0.884	0.0034	29
	MG-50S50F	0.0184	0.00003	1.52	0.0061	30.1
	MG-75S25F	0.021	0.00003	2.68	0.0097	30.4
	MG-100S0F	0.024	0.00003	3.19	0.019	31
3.75	CG-0S100F	0.0470	0.00004	2	0.0199	23
	CG-50S50F	0.0510	0.00007	3.47	0.0211	23
	CG-57S25F	0.0600	0.00008	5.55	0.05	23
	CG-100S0F	0.0660	0.00008	6.04	0.052	23.3
	MG-0S100F	0.0200	0.00003	1.94	0.0062	31
	MG-50S50F	0.0310	0.00004	2.36	0.0073	31.7
	MG-75S25F	0.0390	0.00004	3.74	0.018	32
	MG-100S0F	0.0520	0.00005	4.1	0.0398	32.4

3.2. Rheological properties

3.2.1. Initial apparent viscosity

Grouts must have low initial apparent viscosity to ensure suitable initial fluidity and spreading ability. The initial apparent viscosity values of CG and MG grouts with slag content and molarity are presented in Figs. 4 and 5. Therefore, the initial apparent viscosity of grout at about 500 s^{-1} was selected to establish the estimation of initial apparent viscosity because shear rates <500 s^{-1} have not been able to draw the flow chart [72]. The activation method (mechanochemical activation) affected the initial apparent viscosity of grout. Therefore, the initial apparent viscosity of MG grout samples showed a reduction by 57%, 39%, 35%, and 21% for MG-0S100F, MG-50S50F, MG-75S25F, and MG-100S0F, respectively, in comparison to all CG grout samples (Fig. 4c). It's important to mention that the MG grout had a much higher temperature than CG grout after mixing with water; this is due to the fact that MG powder directly mixed with water and its highest temperature reached around 32 °C in the first 10 min, whereas the alkaline activator based-CG prepared before 24 h of mixing and its highest temperature reached around 62 °C in the first 20 min and maintained above 28 °C for over 8 h. Then, it cooled down slowly to the temperature room (23 °C), after that mixed with the raw materials to produce CG grout. Also, the chemical species of alkaline materials (in solid form) in MG were brought to a lower energy state when dissolved with water and released much more heat to the surroundings. Those species were Na^+ and OH^- for sodium hydroxide and $2Na^{2+} + SiO_2((OH)_2)^{2-}$ for sodium silicate [90]. As a result, increasing the initial temperature of the grout, as shown in Table 3, leads to an increase in the conductivity of the MG grout and the mobility of ions because it solidified much more rapidly than those that appeared in CG grout by the intensive hydration reaction of the raw material, alkaline solids, and water. Thus, it caused an increase in the degree of dissociation in the solution, which in turn is

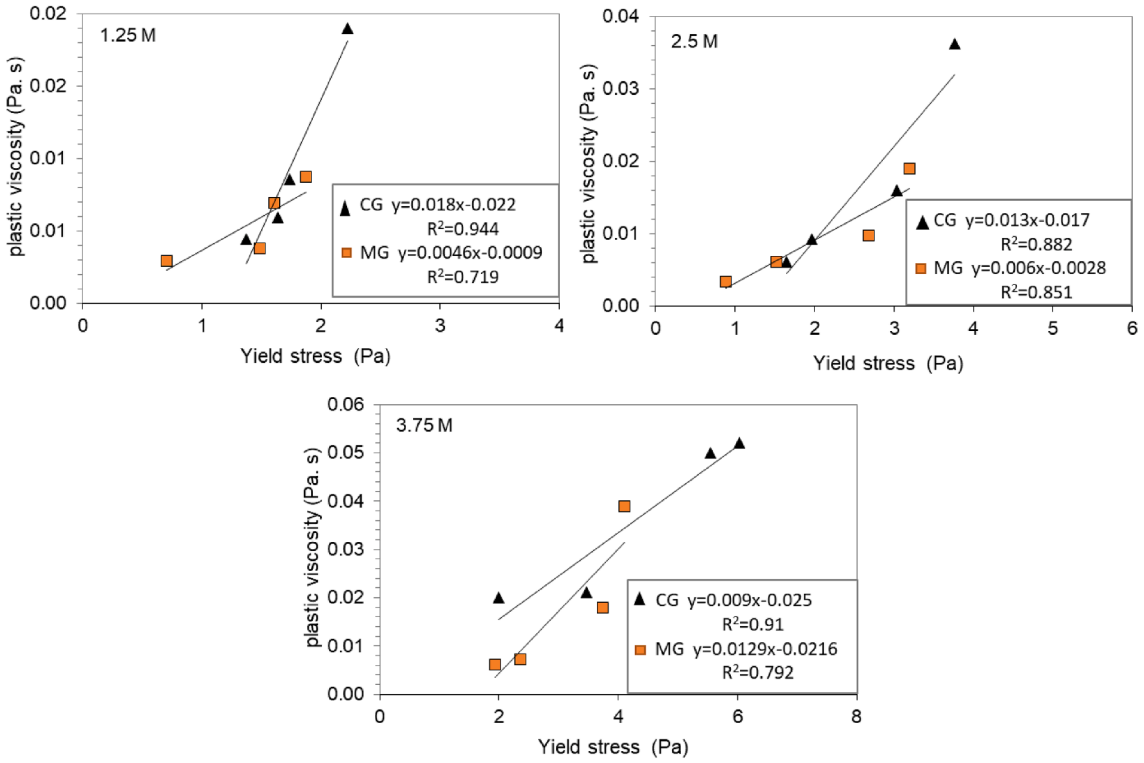

Fig. 6. Relationship between plastic viscosity versus yield stress of MG and CG-based grout.

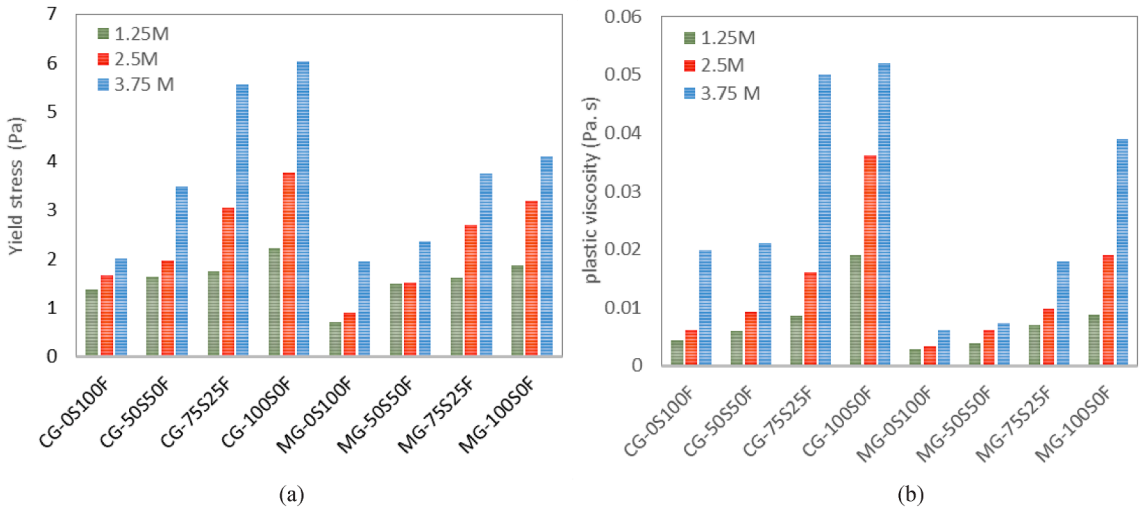

Fig. 7. Influence of molarity of NaOH on the (a) Yield stress and (b) Plastic viscosity of MG and CG - based grout.

responsible for the reduction in the initial viscosity of MG [91]. Similar behavior was reported by Vitola, Laura, et al. [92] and Yang et al. [93].

Generally, the increase in slag content significantly affects the results of apparent viscosity. In other words, increasing slag content leads to a further increase in the apparent viscosity of all mixes regardless of the geopolymer type and molar concentrations. Furthermore, the initial apparent viscosity of MG and CG grouts was dramatically increased with increasing slag content. For example, the apparent viscosity of CG-100S0F and MG-100S0F increased by 40% and 160% compared to the control mixes (CG-0S100F and MG-0S100F), respectively as shown in Fig. 4c. This is attributable to the higher reactivity of slag, resulting in the early formation of primary C-S-H gel [21]. It is well-known that the slag's dissolution is faster than fly ash owing to its higher reaction rate. The ionic bond generated by modifier cations (like Ca^{2+}) and the non-bridging oxygen in the calcium aluminosilicate glass structure is more easily dissolved, resulting in the release of Ca^{2+} ions from slag in the early stage [94]. On other hand, the molar concentration had a major impact on the initial apparent viscosity of CG and MG grouts, as seen in Fig. 5. The higher the molar concentration, the higher initial apparent viscosity despite the grout type; the initial apparent viscosity of CG-100S0F grout increased from 0.0244 to 0.066 Pa.s when the molarity increased from 1.25 M to 3.75 M, respectively. As the concentration of sodium hydroxide increased, the low viscosity stage was shorter, and then the viscosity increased quickly to the initial coagulation, followed

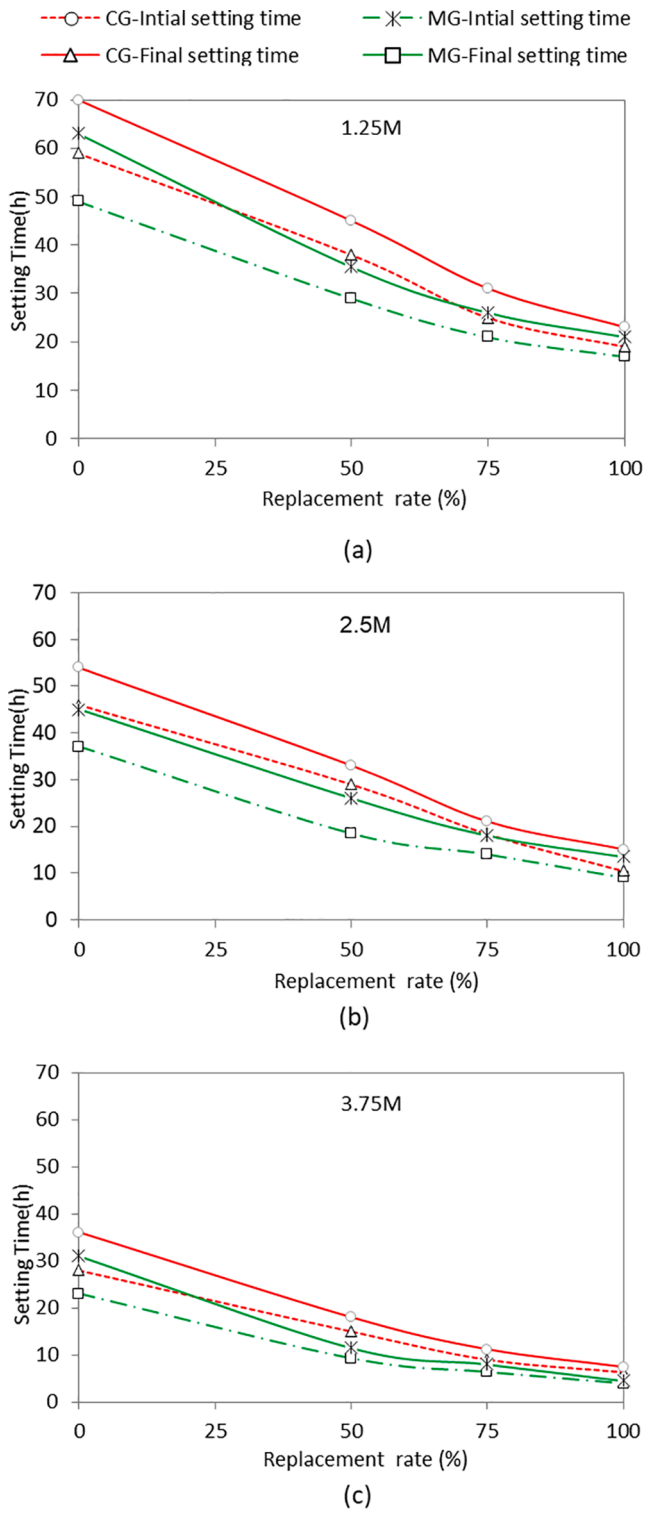

Fig. 8. Setting time of MG and CG - based grout (a) 1.25 M; (b) 2.5 M; (c) 3.75 M.

by fast thickening. Also, the low molarity negatively affected initial apparent viscosity; this could be ascribed to the slow leaching reaction and the low amounts of Si^{4+} and Al^{3+} at low molar concentrations [95].

3.2.2. Yield stress and plastic viscosity

The properties of the rheological tests of the plastic viscosity and yield stress of MG and CG grouts were analyzed according to the modified Bingham model as presented in Table 3. Shear thickening behavior ($C > 0$) was observed for both MG and CG grout mixtures. In other words, based on the C values, the flow behavior of all grouts regardless of the type of activation method exhibited dilatant behavior which means that the viscosity increases with increasing shear rate as shown in Fig. 4. The results indicated that the activation method predominantly influenced the rheological properties of geopolymer grout. The MG grout showed a lower yield stress and plastic viscosity compared to the CG grout, as presented in Table 3. The yield stress and plastic viscosity of MG grout are ranging from 0.701 – 4.1 Pa and 0.0029–0.0389 Pa. s, respectively. The yield stress of CG grout has been varied from 1.37 to 6.04 Pa, and plastic viscosity ranges between 0.0044 and 0.052 Pa.s. This may be attributed to fact that the alkali activator solution would be dissolved rapidly when be mixed with the source materials at very early stages to form conventional geopolymer grout which is much more viscous than water that used to synthesis MG grout, leading to higher yield stress and plastic viscosity of the CG grout. It has been commonly accepted that the viscosity of a suspension increased with the increase of the viscosity of the suspending liquid [96]. The higher yield stress and plastic viscosity of CG grout would be also a disadvantage over MG grout when used as soil injection because it was not easy to pump through the pipe if the materials are too viscous. Therefore, to apply the CG grout in soil injection, measures should be taken to decrease the yield stress and viscosity. Moreover, the low yield stress and plastic viscosity of MG grout may be related to the increase in heat emitted after adding water to MG powder, as shown in Table 3. The initial temperature of MG increased approximately by 35% in comparison with CG grout (23 °C). As mentioned previously in section 3.2.1, the increase in initial temperature increased the dissolution process of geopolymer grout, and the number of ions in a solution increased with the increasing the initial temperature of MG grout, and dissociation increases since the bonds in the electrolyte molecules are activated, resulting in low yield stress and plastic viscosity [92]. Further investigations must be conducted to thoroughly assess the effect of the increase in the initial temperature on the rheological properties of MG grout.

The effects of the activation method of CG and MG grouts under different molarities on the relationship between plastic viscosity versus yield stress are presented in Fig. 6. The relationship between the yield stress and plastic viscosity could also be a beneficial factor for adjusting the pumping pressure and pumping rate during grouting. As seen in Fig. 6, the CG grout has a better correlation coefficient ($0.882 < R^2 < 0.944$) than the MG grout ($0.719 < R^2 < 0.851$). From these relationships, it's noteworthy to mention that the pumping process of CG grout could be more controlled as compared with its counterpart of MG grout. However, an emphasis should be given that the plastic viscosity could influence the pumping process more than the yield stress [97]. In other words, the shear stress (at high shear rates) is gradually more dominated by the plastic viscosity and dilatant behavior [97]. It is found in some past studies [98,99] that pressure loss during pumping pressure of grout is affected by the dilatant response and plastic viscosity rather than the yield stress.

On the other hand, the obtained results showed that the yield stress and plastic viscosity of the MG and CG grouts significantly increased with increasing molarity of sodium hydroxide and slag content, as presented in Table 3. It can be noted that the increasing trend in yield stress and the plastic viscosity may be due to the effect of particle shape that controlling the rheological properties [100,101] and the accelerated chemical reaction due to the higher slag content, which caused the formation of C-A-S-H gel along with N-A-S-H gel at early duration like the reaction process was accelerated [57]. Moreover, the accelerated solidification rate may be related to the rapid formation of some reactions of the mixture materials through the interaction of Ca^{2+} released from the slag with aluminates and silicates [56,102]. It is essential to mention that the highest plastic viscosity and yield stress were obtained at higher molarity and high slag content (Table 3). As seen in Fig. 7, slag-based geopolymer grout showed higher yield stress and plastic viscosity

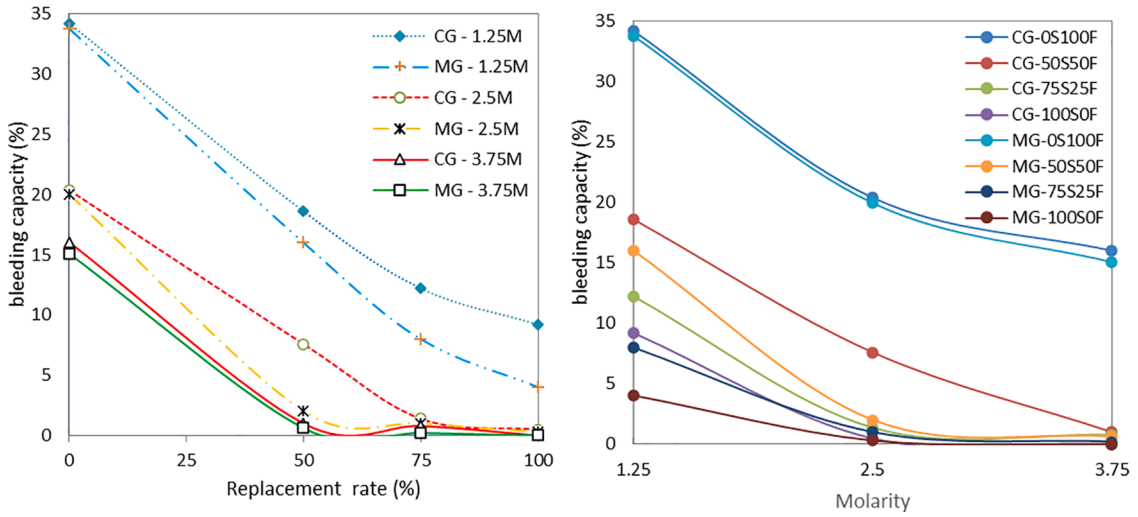

Fig. 9. The bleeding capacity of MG and CG-based grout.

as compared to the fly ash-based geopolymer grout when the molarity of NaOH increased. This behavior is primarily attributable to particle flocculation, which is governed by the shape, and particle size distribution of the precursor is one of the primary causes of viscous behavior. The finer particle size of slag, which promotes particle jamming, enhanced the viscosity of the alkali-activated paste. Particle jamming is a physical process in which the viscosity of materials increases due to increased particle density. In addition, to some extent, the degree of dissolution of the particles, along with the reactivity of the different precursors, influence the viscosity. Also, the incorporation of a high amount of slag binder in geopolymer grout results in significant changes in the reaction products and the physical–chemical interactions. Slag enhances the breakdown and release of silicate and aluminate monomers. The previous studies reported that fly ash possesses low reactivity in producing alkali-activated materials [103,104]. In general, both yield stress and plastic viscosity regardless of the grout type, increased with the increase in molar concentration. The yield stress and plastic viscosity of MG grout are ranging from 0.701–1.87 Pa, and 0.0029–0.00874 Pa.s at a molarity of 1.25 and the range is 1.94–4.1 Pa and 0.0062–0.039 Pa.s at 3.75 M respectively because the interparticle force between sodium hydroxide and sodium silicate may have an effect on the rheological properties [103]. At low molarity, the silicate ions of sodium silicate increased the negative surface charge of the precursor. The adsorption of silicate ions into the precursor (slag or fly ash) resulted in increased interparticle repulsive forces, which caused an increase in the negative surface charge. The increased repulsion between the particles led to deflocculation of the particles and, thus, a lower level of yield stress and plastic viscosity [105]. However, higher molarity is indicative of an increased amount of NaOH in the alkali-activating solution, which results in a greater negative charge of the precursor particles, causing a significant repulsive force, which increases the yield stress of the alkali-activated paste. Moreover, the higher molarity of the alkali-activating solution accelerates the reaction rate of the precursor [106,107]. Similar observations were drawn by Rifaai et al. [81]; the authors studied the influence of sodium hydroxide on the rheology of fly ash-based geopolymer and stated that the concentration of the alkaline activator greatly influences the rheological polymerization process.

3.3. Fresh properties

Grouting is one of the important engineering applications, when using grouting in construction projects, the setting time is an important factor need to be controlled. Due to insufficient duration of setting time, it could cause damage in the machine used for grouting, and on the contrary, long setting time causes a slow construction schedule. Fig. 8 presents the initial and final setting time of MG and CG grouts regarding slag replacement at different molar concentrations. Mechanochemical activation of geopolymer grout has been affected the setting time characteristics. The initial setting time of MG-0S100F, MG-50S50F, MG-75S25F, and MG-100S0F decreased by 18%, 38%, 29%, and 37%, and the final setting time was reduced by 14%, 36%, 29%, and 40% compared to the setting time of CG-0S100F, CG-50S50F, CG-75S25F, and CG-100S0F respectively as shown in Fig. 8c. The results demonstrated that MG grouts had a shorter setting time than CG grouts. This may be due to the mechanochemical activation process creating defects and electronic charges on the surface of the particles, which leads to increased surface energy and crystalline to amorphous phase changes [51]. Additionally, an increase in the surface area and a decrease in particle size will expose a larger surface to a chemical reaction [42,108] resulting in increased particle dissolution, geopolymerization, and reaction rate, which lead to the adsorption of the free mixing water and consequently reduced the setting time of MG grout. Moreover, the mechanochemical activation may have caused a higher proportion of further evenly distributed alumina that came from slag and fly ash, which was enabled to participate and dissolve in geopolymer gel formation [46]. This is attributed to the breakage of large alumino-silicate particles to smaller particles, which increased the surface area and the distribution of particles became more evenly in the mixture [109]. With higher alumino-silicate availability, faster geopolymerization reaction, i.e. formation of aluminosilicate gel occurred, and the gel network eventually included more alumino-silicate components. The resulting gel has a more homogeneous microstructure, presumably due to better crosslinking of alumina and silica [46].

Besides, the increase in slag content significantly affected the setting time duration. As shown in Fig. 8, the setting time of both MG and CG mixtures has been shortened with the increase in slag content. The results showed that the mixes with 100% fly ash (regardless of the geopolymer type) had the longest setting time (Fig. 8a) in contrast to the mixtures with 100% slag that demonstrated the shortest setting time (Fig. 8c). In other words, both the initial and final setting time dramatically reduced with the increase in slag content in both MG and CG mixtures. The initial setting time of MG-50S50F, MG-75S25F, and MG-100S0F was decreased by 59%, 72%, and 83%, and the final setting time was reduced by 63%, 74%, and 85% compared to the setting time of MG-0S100F, respectively. This is mainly attributed to the irregular shape particles and high reactivity of slag compared to fly ash which contributes to the formation of C-A-S-H gel along with N-A-S-H gel at early duration; as such, the reaction process is accelerated [57].

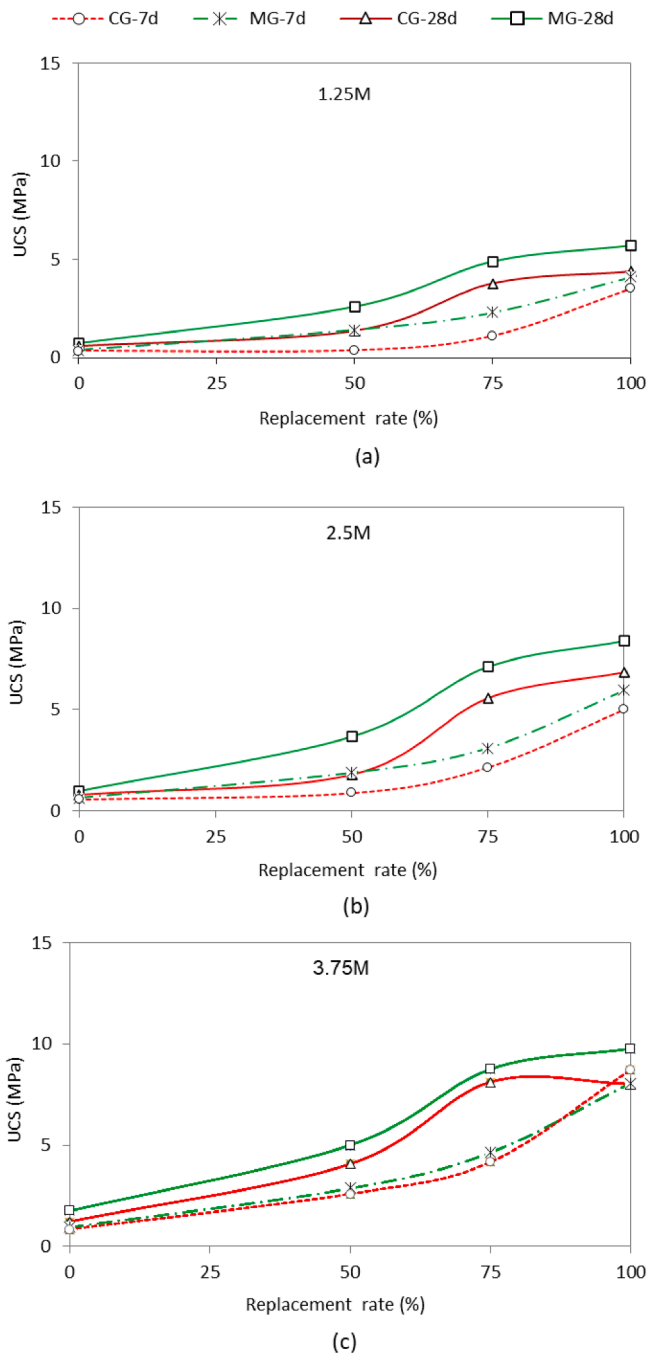

Fig. 10. Unconfined compressive strength (UCS) of MG and CG-based grout, (a) 1.25 M;(b) 2.5 M; (c) 3.75 M.

Moreover, the accelerated solidification rate may be related to the rapid formation of some reactions of the mixture materials through the interaction of Ca^{2+} released from the slag with aluminates and silicates [56,102].

On other hand, the molarity had an apparent effect on the setting time properties of both MG and CG grouts, as seen in Fig. 8. When the molar concentration of NaOH was increased from 1.25 to 2.5, the initial setting time of both MG and CG grouts were increased by 35% and 29%, and the final setting time was increased by 31% and 29 respectively, further decrement was observed when the molarity increased to 3.75 (Fig. 8c). The setting time of MG and CG grouts has been shortened at high molar concentrations. This is attributable to the fact that alkaline conditions accelerate the activation process of geopolymer grout, and the high alkalinity of the NaOH solution leads to the release of Si^{4+}, Al^{3+}, and Ca^{2+} from slag and fly ash, which then diffuse out of the geopolymerization products that form rapidly around the unreacted particles [110].

In addition to the aforementioned results, the bleeding capacity has been conducted in this study to evaluate the variation of bleeding for both MG and CG grouts, as presented in Fig. 9. Generally, geopolymer-based grout is stable if its bleeding capacity is less than 5% beyond the initial coagulation of the slurry [8]. The results demonstrated that the MG grout possessed lower bleeding capacity than that CG regardless of the effect of slag content and molarity. For instance, the bleeding capacity of the MG-75S25F mix was around 33% lower than that CG-75S25F mix. This could be due to the change in the particle size and the increase in the surface area of the powder after the mechanochemical process therefore, more water is needed to cover the surface of particles [46]. From the perspective of slag content, the bleeding capacity of fresh MG and CG grouts was reduced with the increase in slag content therefore, the incorporation of slag can effectively improve the stability of fresh grouts, dissolution heat flow increased with the increase in slag content because slag powder has a higher dissolution than fly ash powder [111], resulting in the quick formation of reaction products to create a rigid network. Specimens with a higher fly ash content have a longer induction period because of the low reaction rate of fly ash. By contrast, the high amount of fly ash negatively increased the bleeding capacity of both MG and CG grouts due to its low water demand and filling effect compared to slag. The fast solidification of slag incorporated mixtures can be attributed to the difference in dissolution and activation kinetics of the fly ash and slag. As reported before [5,56], the accelerated solidification rate may be related to the rapid formation of some reactions of the mixture materials through the interaction of Ca^{2+} released from the slag with aluminates and silicate. Even so, the bleeding capacity of MG and CG grouts decreased with the increase in the molar concentration. It can be seen that the increase of the molarity of NaOH from 1.25 to 2.5 M gradually decreased the bleeding capacity of MG and CG grouts, and the bleeding capacity of both grouts reached the lowest level at 3.75 of molar concentration as shown in Fig. 9. It can be concluded that the molarity of NaOH is an essential factor in the bleeding capacity because as the NaOH concentration increased, the leached amount of Si^{4+} and Al^{3+} increased and more quantity of water was required to perform geopolymer networks. Due to the excessive bleeding capacity which is cause a decrease in grout fluidity, stable geopolymer are recommended [112].

3.4. Mechanical properties

Fig. 10 shows the UCS values of MG and CG specimens versus different slag replacement levels at 7 and 28 days. As seen in Fig. 10, the activation method (mechanochemical activation) has been found to have a pronounced impact on the strength properties of MG samples. The UCS of MG samples showed a strength improvement around 44%, 23%, 8%, and 22% for MG-0S100F, MG-50S50F, MG-75S25F, and MG-100S0F respectively compared with its counterpart of CG samples at 28 days and 3.75 M (Fig. 10c). Mechanochemical activation increased the surface area and the reactivity of slag and fly ash. The reactivity of source materials led to the formation of more gel as the main reaction product, and this gel-filled the pore system. Due to the formation of a larger amount of gel in geopolymer grout, the total pore volume of geopolymer grout was reduced, and porosity was decreased, which in turn is responsible for better immobilization. The pore structure, water, and ions transport determine the resistance of the material to external influences [113]. Also, the diffusion process during leaching depends on pore size distribution [114], stability of the matrix [115], physical properties [116]. Microstructural properties (e,g., porosity, tortuosity, etc.) [117]. Similar behavior of MG grout was reported in [42,51,118,119]. Furthermore, the released heat of MG grout after adding water to MG powder was higher than that of its counterpart of

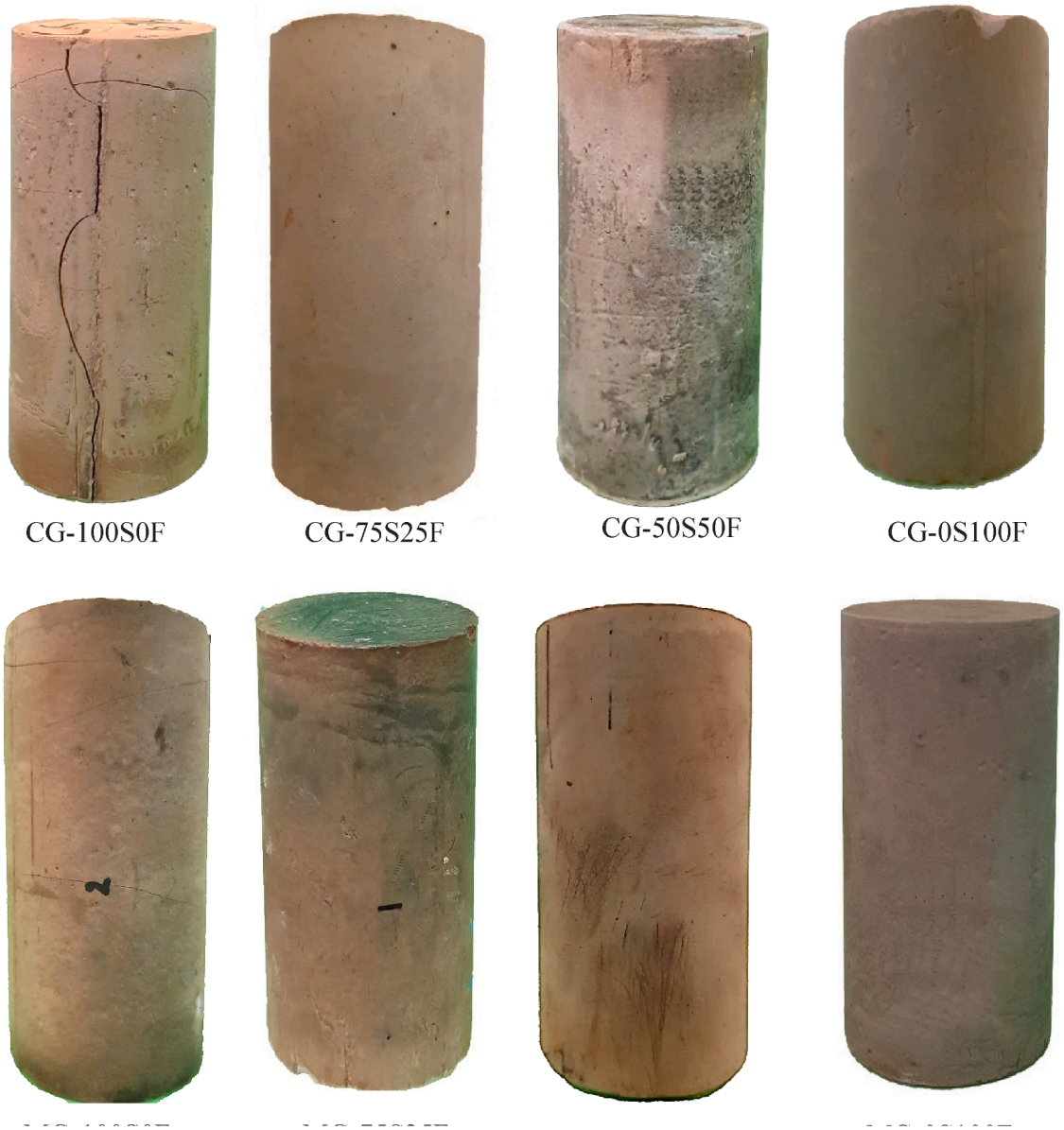

Fig. 11. Surface images of MG and CG-based grout at 3.75 M.

CG grout. MG grout seemed to be slightly hot when hydrated, this advantage could also be an alternative self-heating source for curing purposes of the MG grout, which could accelerate more geopolymeric-gel formation in the matrices and enhancing its mechanical characteristics [31,36]. On other hand, the released temperature of MG grout was low to moderate in this study due to the utilization of low molarities of sodium hydroxide (1.25, 2.5, and 3.75 M); however, if the molarity increased to higher than that of 3.75 M, maybe the released heat during mixing will be higher than 32 °C and will cause micro-pores in geopolymer grout mixture that could give rise to an adverse effect in physical and mechanical properties [36]. In addition to the effect of the activation method, the increase in slag content effectively improved the UCS results; the control samples despite grout type (CG-0S100F and MG-0S100F) exhibited the lowest UCS in comparison with other samples that included different amounts of slag. This can be ascribed to the low reactivity of fly ash compared with slag. The UCS increased gradually with the increase of slag content, the UCS of MG grout increased by 75% when the slag content increased from 50% to 75%, while the UCS of CG grout was also increased by 99% at 28 days and 3.75 M. The remarkable impact of slag on the UCS could be ascribed to better cementing characteristics and higher reactivity compared to fly ash. The high content of CaO plays an essential role in increasing the activation process and early age strength [65]. Furthermore, the high CaO content can produce a C-S-H/CA-S-H gel, thus altering the microstructure of the geopolymer grout mixture and further enhancing the mechanical properties [120]. Also, the formation of C-A-S-H gels would condense the microstructure and reduce the porosity of the geopolymer grout. A similar trend has been reported by Puertas et al. [121], Zhao et al. [122], and Lee and Lee [123], who assessed the effect of the slag amount on strength properties of alkali-activated fly ash/slag based geopolymer concrete; they reported that the compressive strengths increased with the increasing slag content, which in agreement with results of the present investigation.

On other hand, the strength properties of MG and CG grouts were evaluated at different ages, such as 7 and 28 days. It was observed that UCS of all mixtures (except for CG-100S0F) increased with the increasing age because all samples were cured at room temperature and the geopolymerization reaction at these conditions was lower than the samples exposed to heat curing for that reason, the samples with higher

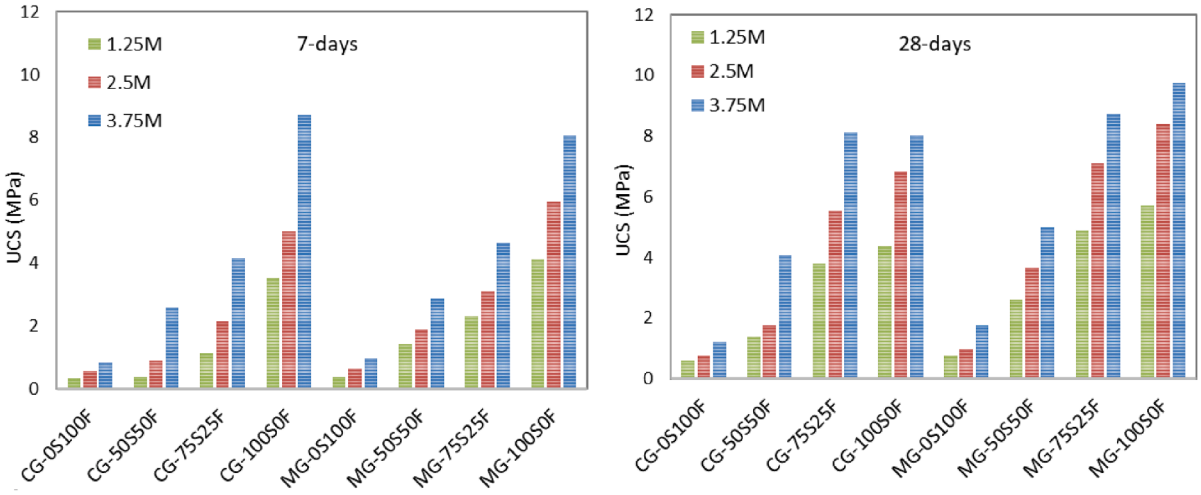

Fig. 12. Influence of molarity of NaOH on the unconfined compressive strength (UCS) of MG and CG-based grout.

age curing (28 days) showed higher strength properties than samples cured at 7 days due to the completion of geopolymerization process at long-ages [124]. Also, the UCS of CG-100S0F samples showed a reduction in strength at 28 days in comparison with the strength of the same samples at 7 days as seen in Fig. 10c. The UCS of CG-100S0F was 8.72 MPa and 8.01 MPa at 7 and 28 days, respectively. Whereas the UCS of MG samples did not experience any reduction in the unconfined compressive strength at 28 days, nonetheless, the UCS of MG samples increased from 8.06 MPa to 9.76 MPa at 28 days. Furthermore, the shape of CG-100S0F samples at 28 days demonstrated apparent cracks on the surface of samples compared to the samples at 7 days, as shown in Fig. 11. The cracks appearance in CG samples with 100% slag content was mainly attributed to the more obvious shrinkage at 28 days than 7 days. The experimental findings demonstrated that higher slag ratios led to higher shrinkage, particularly at long ages of hydration which negatively reduced the UCS of CG grout.

Fig. 12 showed that the molarity of sodium hydroxide significantly affected the UCS results at 7 and 28 days. Generally, the UCS of MG and CG grouts increased with the increase in molar concentration. As seen in Fig. 12, the experimental results showed that the highest UCS was recorded at 3.75 M at all ages and different slag content. For instance, the UCS of CG-75S25F increased by 46% and 114%, while the UCS of MG-75S25F increased by 45% and 79% at 2.5 and 3.75 M at 28 days, respectively when compared to 1.25 M. The enhancement in strength is frequently controlled by the quantity of leached alumino-silicates from the source materials, therefore, the increase in sodium hydroxide concertation leads to higher Si^{4+} and Al^{3+} dissolved, resulting in a strong geopolymeric network. Also, the dissolution at low molarity of NaOH demonstrated that OH^- ions were not sufficient to break the Al-Si bond, which led to producing a few numbers of silicate and aluminate tetrahedral monomers. Whereat OH^- ions at high molarity broke all the Si–Al bonds and formed more silicate and aluminate tetrahedral monomers, and the dissolution was completely done at this stage. Consequently, it condensed the microstructure and improved the mechanical properties of geopolymer grout [125,126]. More, the Na^+ cation balanced the charge deficit of the matrix. Leaching was slow at low alkaline concentration, resulted in a weak polymeric structure, consequently decreased the compressive strength [110].

For validation of unconfined compressive strength results, an ultrasonic pulse velocity (UPV) test was conducted for both MG and CG grouts, as displayed in Fig. 13. It is clear that the UPV values increased with the increased curing time for both MG and CG grouts, and the hardened of all the produced samples categorized between very low velocity to low velocity by UPV values [88]. The results indicated that the activation method had an important role in the UPV values, as seen in Fig. 13. The UPV of MG100S0F, MG75S25F, MG50S50F, and MG0S100F were 1749, 2109, 2280, and 2761 while the UPV of CG100S0F, CG75S25F, CG50S50F, and CG0S100F were 1713, 1912, 2136, and 2686 respectively (Fig. 13c). It can be proved that the mechanochemical process is more advantageous than the traditional activation method in increasing the UPV values because the grinding method of source material decreased the particle size and increased the surface area of fly ash and slag particles which led to reduce the porosity and increased the density of geopolymer grout. Also, the geopolymerization reaction of geopolymer grout significantly increased after the grinding process due to the formation of additional aluminosilicate gel in the mixture, decreasing the porosity and enhancing the reactivity of slag and fly ash particles [42]. Both MG and CG grout showed the highest UPV values among all the studied mixes when the fly ash-based geopolymer grout was fully replaced with a slag binder. This can be related to the increased density of slag-based grout samples compared to the samples of fly ash-based grout, which contributed to reducing the porosity and condense the microstructure of geopolymer grout [57,127,128]. Furthermore, the increase in the molarity of sodium hydroxide was revealed to have a significant effect on the UPV values. In other words, the UPV was found to increase with the increase of the molar concertation, and the highest UPV values were recorded at 3.75 M owing to the high molarity of NaOH solution enhanced the dissolution process of silica and alumina-based source materials, which eventually increased the polycondensation process of geopolymer grout [129]. On other hand, the relationship between the UCS and UPV values for CG and MG grout samples after 28 days is presented in Fig. 14. The MG grout has a higher correlation coefficient ($0.886 < R^2 < 0.968$) than the CG grout ($0.692 < R^2 < 0.916$). The results reveal a strong correlation between UCS and UPV of geopolymer grout (except for the CG grout with 3.75 M).

In this study, the variation in bulk density for both MG and CG grouts was assessed, as shown in Fig. 15. The results showed that MG samples exhibited a higher density than samples of CG grout. In general, the density of MG samples was 4 %, higher than CG. The high density of MG samples was due to the effect of the ball-milling of slag /fly ash and chemical powder (sodium metasilicate and sodium hydroxide) which led to an increase in the surface area and the reactivity of geopolymer grout. Increased reactivity of source materials led to the formation of more gel as the main reaction product, which reduced the porosity and increased the density of MG grout [130]. Also, slag replacement played a vital role in increasing the density of both MG and CG grouts. The density effectively increased with the increase in slag content, the samples with the 100% slag showed the highest density among all the mixes compared with the samples of fly ash-based geopolymer grout.

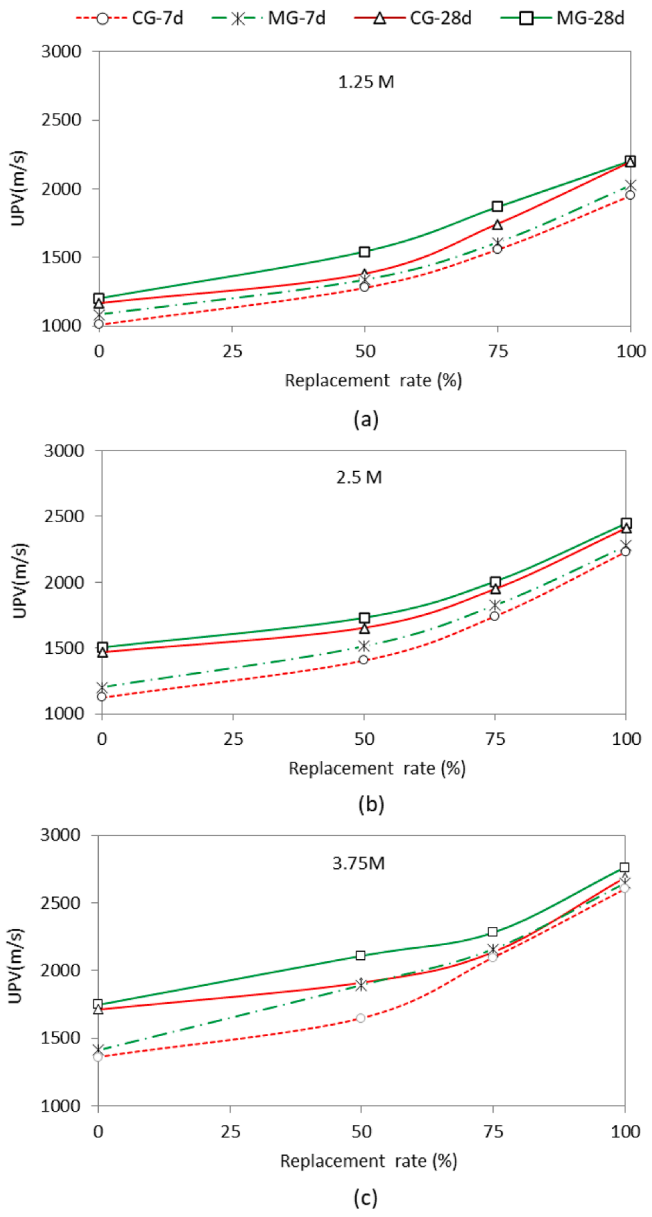

Fig. 13. Ultrasonic pulse velocity (UPV) of MG and CG-based grout, (a) 1.25 M; (b) 2.5 M; (c) 3.75 M.

This is mainly because slag possesses a higher specific gravity (2.9) than fly ash (2.2).

Similar to the results of UCS and UPV, the bulk density of MG and CG grouts increased with the increase in molar concentration of sodium hydroxide, as shown in Fig. 15. Generally, the density of MG grout increased by 5% and 11% at 2.5 and 3.75 M compared to control samples (1.25 M). Similar behavior was detected for the CG grout. The results demonstrated that low molar concentration contributed to a low density for geopolymer grout as it contained a lower NaOH concentration. Normally, an increment in the density of geopolymer grout is accompanied by an increase in the impact strength. Because of the high concentration of NaOH solution, it produces a greater dissolution process from the leaching of silica and alumina. This great dissolution process will contribute to the increase in geopolymerization reaction [129]. Similar results were reported by Abdullah et al. [125], and they showed that the dissolution at low molarity of NaOH demonstrated that OH^- ions are not sufficient to break the Al-Si bond, which led to producing a few numbers of silicate and aluminate tetrahedral monomers. Whereas OH^- ions at high molarity broke all the Si–Al bonds and formed more silicate and aluminate tetrahedral monomers and the dissolution was completely done at this stage, consequently condensed the microstructure and improved the mechanical properties of geopolymer grout.

4. Conclusions

This study aimed to investigate the behavior of mechanochemical activation of geopolymer grout in comparison with the conventional activation of geopolymer grout. The effect of slag to fly ash ratio and the molarity of sodium hydroxide of both MG and CG grouts were assessed through rheological properties (yield stress and plastic viscosity), fresh properties (bleeding and setting time), mechanical properties (unconfined compressive strength and ultrasonic pulse velocity), and microstructure properties (scanning electron microscopy analysis). The conclusions were as follows:

- The results proved that the mechanochemical activation of geopolymer grout was safer and easier to handle than the conventional activation because it eliminated the use of hazardous alkali activator solution.
- The SEM results showed that the particles size of MG powder was reduced, and the shape was slightly changed after grinding, which caused an increase in the surface area of particles that contributed to the formation of additional alumina and silica, which further improved the reactivity of MG powder based-geopolymer grout.
- The activation method (particularly mechanochemical activation) significantly affected the initial apparent viscosity of geopolymer grout. Therefore, the initial apparent viscosity of MG samples demonstrated a reduction approximately by 38% less than that samples of CG grout at the same conditions. Also, the increase in slag content and molar concentration significantly increased the initial apparent viscosity of all geopolymer grouts despite the activation method.
- Both MG and CG grout mixes exhibited shear thickening behavior (increasing apparent viscosity with increasing shear rate), and the yield stress and plastic viscosity of MG and CG grouts generally increased with increasing slag content and molarity. Furthermore, mechanochemical activation has a considerable influence on the rheological characteristics of geopolymer grout compared to the behavior of conventional geopolymer grout. The MG grout showed a lower yield stress and plastic viscosity than the CG grout. The yield stress and plastic viscosity of MG grout are 0.701–4.1 Pa and 0.0029–0.0389 Pa. s, respectively while CG grout has yield stress ranging from 1.37 to 6.04 Pa and a viscosity of 0.0044–0.052 Pa.s.
- Setting time was significantly affected by activation method, slag content, and molarity. The obtained results exhibited that the MG grout had 24.5%, and 20% shorter initial and final setting time as compared with the CG grout respectively. Also, the setting time decreased with the increase in slag content and molarity of sodium hydroxide.
- The bleeding capacity of MG grout was 34% lower than that CG grout which means that the particle size was reduced and the surface area was increased due to the mechanochemical activation mechanism. Also, the bleeding capacity of all the mixtures, regardless of the activation method, decreased with the increase in slag content and molar concentration.
- The experimental results indicated that the unconfined compressive strength of the MG grout was higher than the CG grout. The UCS of MG-0S100F, MG-50S50F, MG-75S25F- and MG-100S0F increased by 44%, 23%, 8%, and 22% in comparison with its counterpart of CG grout at the same conditions. This increment was attributed to the increase in surface area or reduction in particle size of raw materials due to the effect of mechanochemical grinding.
- The obtained results showed that the increase in slag content greatly impacted the mechanical properties of geopolymer grout. The UCS

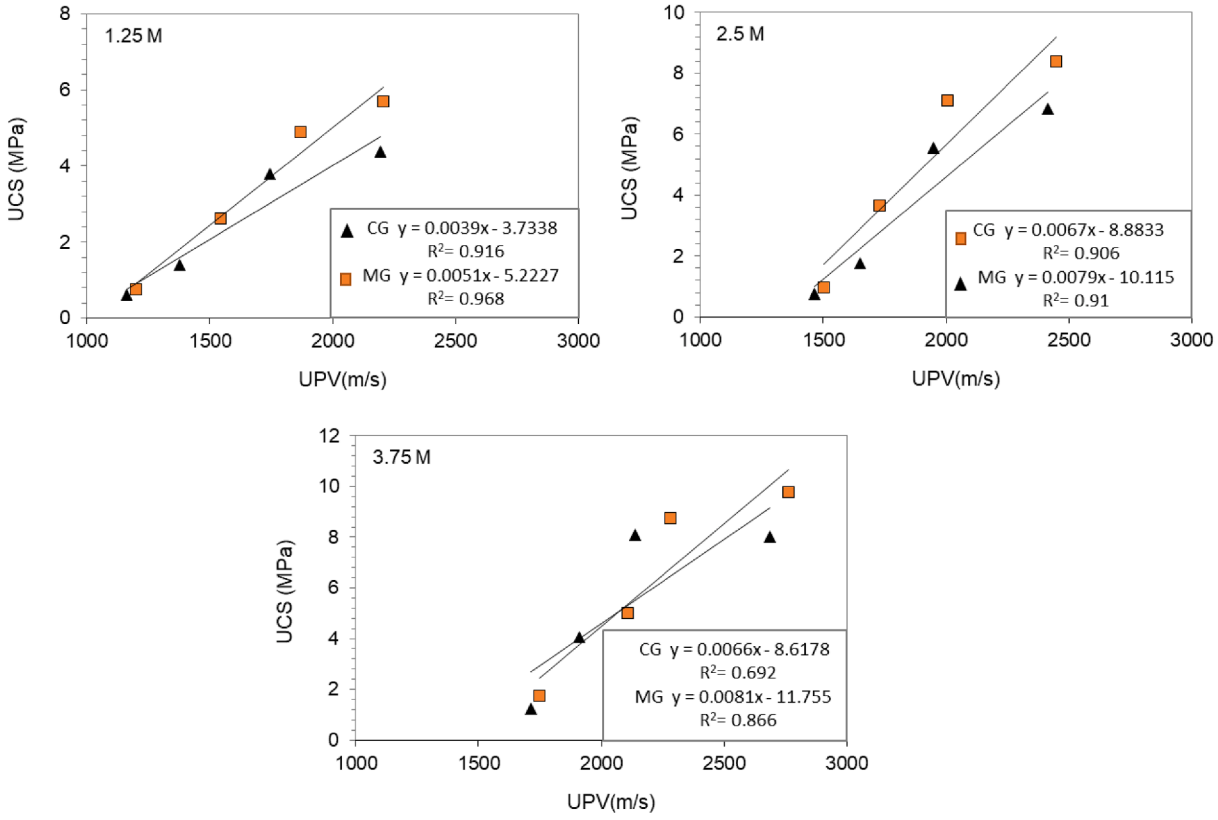

Fig. 14. Correlations of UCS versus UPV of MG and CG - based grout.

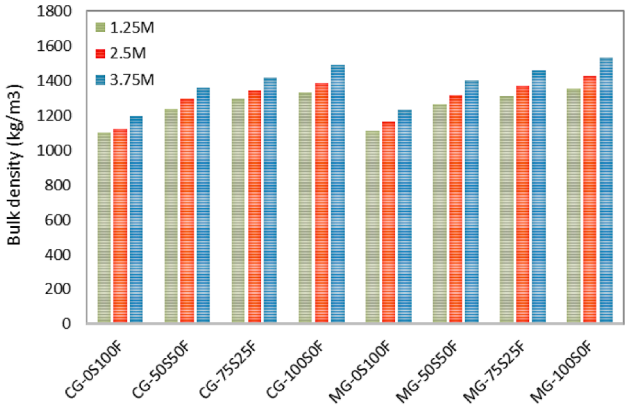

Fig. 15. The bulk density of MG and CG-based grout.

increased gradually with the increasing slag content thus, UCS of MG grout increased by 75% when the slag content increased from 50%–75% and 12% when the slag increased from 75%–100% at 28 days. Also, the UCS of both MG and CG grouts increased with the increasing molarity of sodium hydroxide owing to the increase in sodium hydroxide concertation leads to higher Si^{4+} and Al^{3+} dissolved, resulting in a strong geopolymeric network.

5. Recommendations

- More in-depth investigations must be conducted to thoroughly assess the effect of an increase in the initial temperature on the rheological properties of mechanochemical activation geopolymer grout.
- Further researches should be conducted to evaluate the influence of sodium silicate to sodium hydroxide ratios on the rheological, fresh, and mechanical characteristics of mechanochemical activation geopolymer grout incorporating natural and artificial pozzolans.

CRediT authorship contribution statement

Mukhtar Hamid Abed: Investigation & writing. **Israa Sabbar Abbas:** Data curation. **Majid Hamed:** Review & editing. **Hanifi Canakci:** Supervision.

Declaration of Competing Interest

The authors declare that they have no known competing financial interests or personal relationships that could have appeared to influence the work reported in this paper.

References

[1] H. MR, Engineering Principles of Ground Modifications, (1990).
[2] J. Warner, Practical Handbook of Grouting: Soil, Rock, and Structures, John Wiley & Sons, 2004.
[3] D.P. Coduto, Geotechnical engineering: principles and practices, 1999.
[4] J.L. Provis, P. Duxson, J.S.J. van Deventer, The role of particle technology in developing sustainable construction materials, Adv. Powder Technol. 21 (1) (2010) 2–7.
[5] J.L. Provis, S.A. Bernal, Geopolymers and related alkali-activated materials, Annu. Rev. Mater. Res. 44 (1) (2014) 299–327.
[6] M. Pourabbas Bilondi, M.M. Toufigh, V. Toufigh, Experimental investigation of using a recycled glass powder-based geopolymer to improve the mechanical behavior of clay soils, Constr. Build. Mater. 170 (2018) 302–313.
[7] A. Aboulayt, R. Jaafri, H. Samouh, A.C. El Idrissi, E. Roziere, R. Moussa, A. Loukili, Stability of a new geopolymer grout: rheological and mechanical performances of metakaolin-fly ash binary mixtures, Constr. Build. Mater. 181 (2018) 420–436.

[8] H. Güllü, A. Ali Agha, The rheological, fresh and strength effects of cold-bonded geopolymer made with metakaolin and slag for grouting, Constr. Build. Mater. 274 (2021) 122091. doi:10.1016/j.conbuildmat.2020.122091.

[9] M.M. Ahmed, K.A.M. El-Naggar, D. Tarek, A. Ragab, H. Sameh, A.M. Zeyad, B. A. Tayeh, I.M. Maafa, A. Yousef, Fabrication of thermal insulation geopolymer bricks using ferrosilicon slag and alumina waste, Case Stud. Constr. Mater. 15 (2021), e00737, https://doi.org/10.1016/j.cscm.2021.e00737.

[10] M. Albitar, M.S. Mohamed Ali, P. Visintin, M. Drechsler, Durability evaluation of geopolymer and conventional concretes, Constr. Build. Mater. 136 (2017) 374–385.

[11] R.N. Thakur, S. Ghosh, Effect of mix composition on compressive strength and microstructure of fly ash based geopolymer composites, ARPN J. Eng. Appl. Sci. 4 (2009) 68–74.

[12] A. Islam, U.J. Alengaram, M.Z. Jumaat, I.I. Bashar, S.M.A. Kabir, Engineering properties and carbon footprint of ground granulated blast-furnace slag-palm oil fuel ash-based structural geopolymer concrete, Constr. Build. Mater. 101 (2015) 503–521.

[13] A.M.A. Blash, T.V.S.V. Lakshmi, Properties of geopolymer concrete produced by silica fume and ground-granulated blast-furnace slag, Int. J. Sci. Res. 5 (2016) 319–323.

[14] H. Xu, W. Gong, L. Syltebo, K. Izzo, W. Lutze, I.L. Pegg, Effect of blast furnace slag grades on fly ash based geopolymer waste forms, Fuel. 133 (2014) 332–340.

[15] J.J.A. Baldovino, R.L.S. Izzo, J.L. Rose, M.D.I. Domingos, Strength, durability, and microstructure of geopolymers based on recycled-glass powder waste and dolomitic lime for soil stabilization, Constr. Build. Mater. 271 (2021), 121874.

[16] A.L. Almutairi, B.A. Tayeh, A. Adesina, H.F. Isleem, A.M. Zeyad, Potential applications of geopolymer concrete in construction: a review, Case Stud. Constr. Mater. 15 (2021), e00733, https://doi.org/10.1016/j.cscm.2021.e00733.

[17] M. Amin, A.M. Zeyad, B.A. Tayeh, I.S. Agwa, Effect of high temperatures on mechanical, radiation attenuation and microstructure properties of heavyweight geopolymer concrete, Struct. Eng. Mech. 80 (2021) 181–199.

[18] A. Favier, J. Hot, G. Habert, N. Roussel, J.B. D'Espinose De Lacaillerie, Flow properties of MK-based geopolymer pastes. A comparative study with standard Portland cement pastes, Soft Matter. 10 (2014) 1134–1141, https://doi.org/10.1039/c3sm51889b.

[19] F. Pacheco-Torgal, D. Moura, Y. Ding, S. Jalali, Composition, strength and workability of alkali-activated metakaolin based mortars, Constr. Build. Mater. 25 (9) (2011) 3732–3745.

[20] F. Pacheco-Torgal, J. Castro-Gomes, S. Jalali, Alkali-activated binders: A review. Part 2. About materials and binders manufacture, Constr. Build. Mater. 22 (2008) 1315–1322.

[21] M. Palacios, P.F.G. Banfill, F. Puertas, Rheology and setting of alkali-activated slag pastes and mortars: effect of organic admixture, ACI Mater. J. 105 (2008) 140.

[22] A. Çevik, R. Alzeebaree, G. Humur, M. Eren, E ff ect of nano-silica on the chemical durability and mechanical performance of fl y ash based geopolymer concrete, 44 (2018) 12253–12264. doi:10.1016/j.ceramint.2018.04.009.

[23] S.M.S. Taher, S.T. Saadullah, J.H. Haido, B.A. Tayeh, Behavior of geopolymer concrete deep beams containing waste aggregate of glass and limestone as a partial replacement of natural sand, Case Stud. Constr. Mater. 15 (2021), e00744, https://doi.org/10.1016/j.cscm.2021.e00744.

[24] B.A. Tayeh, A.M. Zeyad, I. Saad, M. Amin, Effect of elevated temperatures on mechanical properties of lightweight geopolymer concrete, Case Stud. Constr. Mater. 15 (2021), e00673, https://doi.org/10.1016/j.cscm.2021.e00673.

[25] W.K.W. Lee, J.S. J, Structural reorganisation of class F fly ash in alkaline silicate solutions, 211 (2002) 49–66.

[26] W.K.W. Lee, J.S.J. van Deventer, Use of Infrared Spectroscopy to Study Geopolymerization of Heterogeneous Amorphous Aluminosilicates, Langmuir. 19 (21) (2003) 8726–8734, https://doi.org/10.1021/la026127e.

[27] P. Duxson, J.L. Provis, Designing precursors for geopolymer cements, J. Am. Ceram. Soc. 91 (2008) 3864–3869, https://doi.org/10.1111/j.1551-2916.2008.02787.x.

[28] J.L. Provis, Activating solution chemistry for geopolymers, Geopolym. Struct. Process. Prop. Ind. Appl. (2009) 50–71, https://doi.org/10.1533/9781845696382.1.50.

[29] M. Criado, A. Fernández-Jiménez, A.G. de la Torre, M.A.G. Aranda, A. Palomo, An XRD study of the effect of the SiO2/Na2O ratio on the alkali activation of fly ash, Cem. Concr. Res. 37 (5) (2007) 671–679.

[30] E. Najafi Kani, A. Allahverdi, J.L. Provis, Efflorescence control in geopolymer binders based on natural pozzolan, Cem. Concr. Compos. 34 (1) (2012) 25–33.

[31] G. Masi, A. Filipponi, M.C. Bignozzi, Fly ash-based one-part alkali activated mortars cured at room temperature: effect of precursor pre-treatments, Open Ceram. 8 (2021), 100178, https://doi.org/10.1016/j.oceram.2021.100178.

[32] X. Ke, S.A. Bernal, N. Ye, J.L. Provis, J. Yang, J. Biernacki, One-part geopolymers based on thermally treated red mud/NaOH blends, J. Am. Ceram. Soc. 98 (1) (2015) 5–11.

[33] S. Muthukrishnan, S. Ramakrishnan, J. Sanjayan, Effect of alkali reactions on the rheology of one-part 3D printable geopolymer concrete, Cem. Concr. Compos. 116 (2021), 103899, https://doi.org/10.1016/j.cemconcomp.2020.103899.

[34] B. Nematollahi, J. Sanjayan, F.U.A. Shaikh, Synthesis of heat and ambient cured one-part geopolymer mixes with different grades of sodium silicate, Ceram. Int. 41 (4) (2015) 5696–5704.

[35] D. Koloušek, J. Brus, M. Urbanova, J. Andertova, V. Hulinsky, J. Vorel, Preparation, structure and hydrothermal stability of alternative (sodium silicate-free) geopolymers, J. Mater. Sci. 42 (22) (2007) 9267–9275.

[36] T. Suwan, M. Fan, Effect of manufacturing process on the mechanisms and mechanical properties of fly ash-based geopolymer in ambient curing temperature, Mater. Manuf. Process. 32 (5) (2017) 461–467, https://doi.org/10.1080/10426914.2016.1198013.

[37] M. Askarian, Z. Tao, B. Samali, G. Adam, R. Shuaibu, Mix composition and characterisation of one-part geopolymers with different activators, Constr. Build. Mater. 225 (2019) 526–537, https://doi.org/10.1016/j.conbuildmat.2019.07.083.

[38] R. Gupta, P. Bhardwaj, D. Mishra, M. Mudgal, R.K. Chouhan, M. Prasad, S. S. Amritphale, Evolution of advanced geopolymeric cementitious material via a novel process, Adv. Cem. Res. 29 (3) (2017) 125–134, https://doi.org/10.1680/jadcr.16.00113.

[39] G. Intini, L. Liberti, M. Notarnicola, F. Di Canio, Mechanochemical activation of coal fly ash for production of high strength cement conglomerates, ХиМия в Интересах Устойчивого Развития. 17 (2009) 567–571.

[40] P. Baláž, M. Achimovičová, M. Baláž, P. Billik, Z. Cherkezova-Zheleva, J. M. Criado, F. Delogu, E. Dutková, E. Gaffet, F.J. Gotor, others, Hallmarks of mechanochemistry: from nanoparticles to technology, Chem. Soc. Rev. 42 (2013) 7571–7637.

[41] A. Souri, H. Kazemi-Kamyab, R. Snellings, R. Naghizadeh, F. Golestani-Fard, K. Scrivener, Pozzolanic activity of mechanochemically and thermally activated kaolins in cement, Cem. Concr. Res. 77 (2015) 47–59.

[42] S. Kumar, R. Kumar, Mechanical activation of fly ash: effect on reaction, structure and properties of resulting geopolymer, Ceram. Int. 37 (2011) 533–541.

[43] G. Mucsi, S. Kumar, B. Csoke, R. Kumar, Z. Molnár, Á. Rácz, F. Mádai, Á. Debreczeni, Control of geopolymer properties by grinding of land filled fly ash, Int. J. Miner. Process. 143 (2015) 50–58, https://doi.org/10.1016/j.minpro.2015.08.010.

[44] S. Kumar, F. Kristály, G. Mucsi, Geopolymerisation behaviour of size fractioned fly ash, Adv. Powder Technol. 26 (1) (2015) 24–30.

[45] J. Temuujin, R.P. Williams, A. van Riessen, Effect of mechanical activation of fly ash on the properties of geopolymer cured at ambient temperature, J. Mater. Process. Technol. 209 (12-13) (2009) 5276–5280.

[46] N. Marjanović, M. Komljenović, Z. Baščarević, V. Nikolić, Improving reactivity of fly ash and properties of ensuing geopolymers through mechanical activation, Constr. Build. Mater. 57 (2014) 151–162.

[47] R. Gupta, P. Bhardwaj, K. Deshmukh, D. Mishra, M. Prasad, S.S. Amritphale, Development and Characterization of Inorganic-Organic (Si-O-Al) Hybrid Geopolymeric Precursors via Solid State Method, Silicon. 11 (1) (2019) 221–232.

[48] A.T. Almalkawi, A. Balchandra, P. Soroushian, Potential of using industrial wastes for production of geopolymer binder as green construction materials, Constr. Build. Mater. 220 (2019) 516–524.

[49] R. Gupta, P. Bhardwaj, D. Mishra, M. Prasad, S.S. Amritphale, Formulation of mechanochemically evolved fly ash based hybrid inorganic–organic geopolymers with multilevel characterization, J. Inorg. Organomet. Polym. Mater. 27 (2) (2017) 385–398.

[50] M. Mudgal, R.K. Chouhan, S. Kushwah, A.K. Srivastava, Enhancing reactivity and properties of fl y-ash-based solid-form geopolymer via, Eng. Mater. Res. 9 (2020) 1–8.

[51] S. Hosseini, N.A. Brake, M. Nikookar, Ö. Günaydın-Şen, H.A. Snyder, Mechanochemically activated bottom ash-fly ash geopolymer, Cem. Concr. Compos. 118 (2021), https://doi.org/10.1016/j.cemconcomp.2021.103976.

[52] P. Duxson, A. Fernández-Jiménez, J.L. Provis, G.C. Lukey, A. Palomo, J.S.J. Van Deventer, Geopolymer technology: the current state of the art, J. Mater. Sci. 42 (2007) 2917–2933, https://doi.org/10.1007/s10853-006-0637-z.

[53] D. Panias, I.P. Giannopoulou, T. Perraki, Effect of synthesis parameters on the mechanical properties of fly ash-based geopolymers, Colloids Surfaces A Physicochem. Eng. Asp. 301 (1-3) (2007) 246–254, https://doi.org/10.1016/j.colsurfa.2006.12.064.

[54] M. Komljenovic, Z. Miladinovic, V. Nikolic, Z. Zoran, Effects of the concentrated NH 4 NO 3 solution on mechanical properties and structure of the fly ash based geopolymers ˙arevic, 41 (2013) 570–579. doi:10.1016/j.conbuildmat.2012.12.067.

[55] F. Winnefeld, A. Leemann, M. Lucuk, P. Svoboda, M. Neuroth, Assessment of phase formation in alkali activated low and high calcium fly ashes in building materials, Constr. Build. Mater. 24 (6) (2010) 1086–1093, https://doi.org/10.1016/j.conbuildmat.2009.11.007.

[56] S. Samantasinghar, S.P. Singh, Fresh and hardened properties of fly ash-slag blended geopolymer paste and mortar, Int. J. Concr. Struct. Mater. 13 (2019) 1–12, https://doi.org/10.1186/s40069-019-0360-1.

[57] S. Kumar, R. Kumar, S.P. Mehrotra, Influence of granulated blast furnace slag on the reaction, structure and properties of fly ash based geopolymer, J. Mater. Sci. 45 (3) (2010) 607–615, https://doi.org/10.1007/s10853-009-3934-5.

[58] N. Marjanović, M. Komljenović, Z. Baščarević, V. Nikolić, R. Petrović, Physical-mechanical and microstructural properties of alkali-activated fly ash-blast furnace slag blends, Ceram. Int. 41 (1) (2015) 1421–1435, https://doi.org/10.1016/j.ceramint.2014.09.075.

[59] M. Palacios, S. Gismera, M.M. Alonso, J.B. d'Espinose de Lacaillerie, B. Lothenbach, A. Favier, C. Brumaud, F. Puertas, Early reactivity of sodium silicate-activated slag pastes and its impact on rheological properties, Cem. Concr. Res. 140 (2021), 106302, https://doi.org/10.1016/j.cemconres.2020.106302.

[60] C. Lu, Z. Zhang, C. Shi, N. Li, D. Jiao, Q. Yuan, Rheology of alkali-activated materials: a review, Cem. Concr. Compos. 121 (2021) 104061, https://doi.org/10.1016/j.cemconcomp.2021.104061.

[61] H. Ye, A. Radlińska, Shrinkage mitigation strategies in alkali-activated slag, Cem. Concr. Res. 101 (2017) 131–143, https://doi.org/10.1016/j.cemconres.2017.08.025.

[62] H. Ye, A. Radlińska, Shrinkage mechanisms of alkali-activated slag, Cem. Concr. Res. 88 (2016) 126–135, https://doi.org/10.1016/j.cemconres.2016.07.001.

[63] M. Hojati, A. Radlińska, Shrinkage and strength development of alkali-activated fly ash-slag binary cements, Constr. Build. Mater. 150 (2017) 808–816, https://doi.org/10.1016/j.conbuildmat.2017.06.040.

[64] S. Puligilla, P. Mondal, Role of slag in microstructural development and hardening of fl y ash-slag geopolymer, Cem. Concr. Res. 43 (2013) 70–80, https://doi.org/10.1016/j.cemconres.2012.10.004.

[65] S.K. Nath, S. Kumar, Influence of iron making slags on strength and microstructure of fly ash geopolymer, Constr. Build. Mater. 38 (2013) 924–930, https://doi.org/10.1016/j.conbuildmat.2012.09.070.

[66] J.G. Jang, N.K. Lee, H.K. Lee, Fresh and hardened properties of alkali-activated fly ash/slag pastes with superplasticizers, Constr. Build. Mater. 50 (2014) 169–176, https://doi.org/10.1016/j.conbuildmat.2013.09.048.

[67] P. Bhardwaj, R. Gupta, D. Mishra, S.K. Sanghi, S. Verma, S.S. Amritphale, Corrosion and fire protective behavior of advanced phosphatic geopolymeric coating on mild steel substrate, Silicon. 12 (3) (2020) 487–500, https://doi.org/10.1007/s12633-019-00153-1.

[68] R. Gupta, A.S. Tomar, D. Mishra, S.K. Sanghi, Multinuclear MAS NMR Characterization of Fly-Ash-based advanced sodium aluminosilicate geopolymer: exploring solid-state reactions, ChemistrySelect. 5 (2020) 4920–4927, https://doi.org/10.1002/slct.202000203.

[69] M. Mudgal, R.K. Chouhan, S. Kushwah, A.K. Srivastava, Enhancing reactivity and properties of fly-ash-based solid-form geopolymer via ball-milling, Emerg, Mater. Res. 9 (2019) 2–9.

[70] M. Manish, C.R. Kumar, M. Deepti, F. Application, P. Data, (12) United States Patent, 2 (2016).

[71] C. Fluids, Standard test method for viscosity of chemical grouts by brookfield viscometer, Annu. B. ASTM Stand. 04 (2003) 8–10, https://doi.org/10.1520/D4016-08.2.

[72] H. Güllü, A. Cevik, K.M.A. Al-Ezzi, M.E. Gülsan, On the rheology of using geopolymer for grouting: A comparative study with cement-based grout included fly ash and cold bonded fly ash, Constr. Build. Mater. 196 (2019) 594–610.

[73] H. Güllü, M.M.D. Al Nuaimi, A. Aytek, Rheological and strength performances of cold-bonded geopolymer made from limestone dust and bottom ash for grouting and deep mixing, Bull. Eng. Geol. Environ. 80 (2) (2021) 1103–1123, https://doi.org/10.1007/s10064-020-01998-2.

[74] M. Şahmaran, The effect of replacement rate and fineness of natural zeolite on the rheological properties of cement-based grouts, Can. J. Civ. Eng. 35 (8) (2008) 796–806.

[75] A. Yahia, K.H. Khayat, Analytical models for estimating yield stress of high-performance pseudoplastic grout, Cem. Concr. Res. 31 (5) (2001) 731–738.

[76] C.K. Park, M.H. Noh, T.H. Park, Rheological properties of cementitious materials containing mineral admixtures, Cem. Concr. Res. 35 (5) (2005) 842–849.

[77] B. Widjaja, S. Hsien-Heng Lee, Flow box test for viscosity of soil in plastic and viscous liquid states, Soils Found. 53 (1) (2013) 35–46.

[78] A. Yahia, S. Mantellato, R.J. Flatt, Concrete rheology: a basis for understanding chemical admixtures, in: Sci. Technol. Concr. Admixtures, Elsevier, 2016: pp. 97–127.

[79] H. Güllü, Comparison of rheological models for jet grout cement mixtures with various stabilizers, Constr. Build. Mater. 127 (2016) 220–236, https://doi.org/10.1016/j.conbuildmat.2016.09.129.

[80] D. Feys, J.E. Wallevik, A. Yahia, K.H. Khayat, O.H. Wallevik, Extension of the Reiner-Riwlin equation to determine modified Bingham parameters measured in coaxial cylinders rheometers, Mater. Struct. Constr. 46 (1-2) (2013) 289–311, https://doi.org/10.1617/s11527-012-9902-6.

[81] Y. Rifaai, A. Yahia, A. Mostafa, S. Aggoun, E.H. Kadri, Rheology of fly ash-based geopolymer: effect of NaOH concentration, Constr. Build. Mater. 223 (2019) 583–594, https://doi.org/10.1016/j.conbuildmat.2019.07.028.

[82] American Society for Testing & Mater, Standard test methods for felt, (1987) 1–8. doi:10.1520/C0191-19.2.

[83] ASTM:C940-10a, Standard Test Method for Expansion and Bleeding of Freshly Mixed Grouts for Preplaced-Aggregate Concrete in the Laboratory, ASTM Int. i (2010) 1–3. doi:10.1520/C0940-16.2.

[84] F. Celik, H. Canakci, Examination of the mechanical properties and failure pattern of soilcrete mixtures modified with rice husk ash, Eur. J. Environ. Civ. Eng. 24 (8) (2020) 1245–1260.

[85] C.C. Test, C. Ag-, A. Concrete, P. Concrete, StandardTest Method for Compressive Strength of Grouts for Preplaced-Aggregate Concrete in the Laboratory 1, (2021) 10–12.

[86] D. Dimensional, S. Tolerances, Standard Test Method for Unconfined Compressive Strength of Intact Rock Core, 03 (2021) 14–16.

[87] C. ASTM, Standard test method for pulse velocity through concrete, ASTM Int. West Conshohocken, PA. (2009).

[88] O.H. Anon, Classification of rocks and soils for engineering geological mapping. Part 1: rock and soil materials, Bull. Int. Assoc. Eng. Geol. 19 (1979) 355–371.

[89] J. Baalamurugan, V. Ganesh Kumar, T. Stalin Dhas, S. Taran, S. Nalini, V. Karthick, M. Ravi, K. Govindaraju, Utilization of induction furnace steel slag based iron oxide nanocomposites for antibacterial studies, SN, Appl. Sci. 3 (2021) 1–8, https://doi.org/10.1007/s42452-021-04299-9.

[90] W. Sottisopha, S. Asavapisit, Immobilization of the Plating Sludge by Activation of Pulverized Fuel Ash with Sodium Silicate Solution, 10 (2005).

[91] A. Usobiaga, A. de Diego, J.M. Madariaga, Electrical conductivity of concentrated aqueous mixtures of HCl and KCl in a wide range of compositions and temperatures, J. Chem. Eng. Data. 45 (1) (2000) 23–28, https://doi.org/10.1021/je990160u.

[92] L. Vitola, I. Pundiene, J. Pranckeviciene, D. Bajare, The impact of the amount of water used in activation solution and the initial temperature of paste on the rheological behaviour and structural evolution of metakaolin-based geopolymer pastes, Sustain. 12 (2020), https://doi.org/10.3390/su12198216.

[93] X. Yang, W. Zhu, Q. Yang, The viscosity properties of sodium silicate solutions, J. Solution Chem. 37 (1) (2008) 73–83, https://doi.org/10.1007/s10953-007-9214-6.

[94] K.C. Newlands, M. Foss, T. Matchei, J. Skibsted, D.E. Macphee, Early stage dissolution characteristics of aluminosilicate glasses with blast furnace slag- and fly-ash-like compositions, J. Am. Ceram. Soc. 100 (5) (2017) 1941–1955.

[95] J. Zhang, S. Li, Z. Li, Q. Zhang, H. Li, J. Du, Y. Qi, Properties of fresh and hardened geopolymer-based grouts, Ceram. - Silikaty. 63 (2019) 164–173. doi: 10.13168/cs.2019.0008.

[96] B.J. Konijn, O.B.J. Sanderink, N.P. Kruyt, Experimental study of the viscosity of suspensions: effect of solid fraction, particle size and suspending liquid, Powder Technol. 266 (2014) 61–69, https://doi.org/10.1016/j.powtec.2014.05.044.

[97] D. Feys, R. Verhoeven, G. De Schutter, Why is fresh self-compacting concrete shear thickening? Cem. Concr. Res. 39 (6) (2009) 510–523, https://doi.org/10.1016/j.cemconres.2009.03.004.

[98] D. Feys, R. Verhoeven, G. De Schutter, The paradox of self-compacting concrete: why does it require more energy during pumping?, in: 3rd Int. Symp. Non-Traditional Cem. Concr., 2008: pp. 228–236.

[99] D. Feys, R. Verhoeven, G. De Schutter, Full scale pumping tests on SCC: test description and results, in: 3rd North Am. Conf. Des. Use Self-Consolidating Concr. Challenges Barriers to Appl. (SCC 2008), 2009: pp. 631–636.

[100] T. Yang, H. Zhu, Z. Zhang, X. Gao, C. Zhang, Q. Wu, Effect of fly ash microsphere on the rheology and microstructure of alkali-activated fly ash/slag pastes, Cem. Concr. Res. 109 (2018) 198–207, https://doi.org/10.1016/j.cemconres.2018.04.008.

[101] D.P. Bentz, C.F. Ferraris, M.A. Galler, A.S. Hansen, J.M. Guynn, Influence of particle size distributions on yield stress and viscosity of cement-fly ash pastes, Cem. Concr. Res. 42 (2) (2012) 404–409, https://doi.org/10.1016/j.cemconres.2011.11.006.

[102] P. Nath, P.K. Sarker, Effect of GGBFS on setting, workability and early strength properties of fly ash geopolymer concrete cured in ambient condition, Constr. Build. Mater. 66 (2014) 163–171.

[103] M. Palacios, M.M. Alonso, C. Varga, F. Puertas, Influence of the alkaline solution and temperature on the rheology and reactivity of alkali-activated fly ash pastes, Cem. Concr. Compos. 95 (2019) 277–284, https://doi.org/10.1016/j.cemconcomp.2018.08.010.

[104] D. Glosser, P. Suraneni, O.B. Isgor, W.J. Weiss, Estimating reaction kinetics of cementitious pastes containing fly ash, Cem. Concr. Compos. 112 (2020), 103655, https://doi.org/10.1016/j.cemconcomp.2020.103655.

[105] G. Landrou, C. Brumaud, F. Winnefeld, R.J. Flatt, G. Habert, Lime as an anti-plasticizer for self-compacting clay concrete, Materials (Basel). 9 (2016), https://doi.org/10.3390/ma9050330.

[106] S. Hanjitsuwan, S. Hunpratub, P. Thongbai, S. Maensiri, V. Sata, P. Chindaprasirt, Effects of NaOH concentrations on physical and electrical properties of high calcium fly ash geopolymer paste, Cem. Concr. Compos. 45 (2014) 9–14, https://doi.org/10.1016/j.cemconcomp.2013.09.012.

[107] M.B. Karakoç, I. Türkmen, M.M. Maraş, F. Kantarci, R. Demirboła, M. Ułur Toprak, Mechanical properties and setting time of ferrochrome slag based geopolymer paste and mortar, Constr. Build. Mater. 72 (2014) 283–292, https://doi.org/10.1016/j.conbuildmat.2014.09.021.

[108] K. Kato, Y. Xin, T. Hitomi, T. Shirai, Surface modification of fly ash by mechano-chemical treatment, Ceram. Int. 45 (1) (2019) 849–853, https://doi.org/10.1016/j.ceramint.2018.09.254.

[109] H. Li, D. Xu, S. Feng, B. Shang, Microstructure and performance of fly ash microbeads in cementitious material system, Constr. Build. Mater. 52 (2014) 422–427, https://doi.org/10.1016/j.conbuildmat.2013.11.040.

[110] N. Marjanovi, M. Komljenovi, Z. Ba, V. Nikoli, R. Petrovi, Physical – mechanical and microstructural properties of alkali-activated fl y ash – blast furnace slag blends, (2014). doi:10.1016/j.ceramint.2014.09.075.

[111] X. Gao, Q.L. Yu, H.J.H. Brouwers, Reaction kinetics, gel character and strength of ambient temperature cured alkali activated slag-fly ash blends, Constr. Build. Mater. 80 (2015) 105–115, https://doi.org/10.1016/j.conbuildmat.2015.01.065.

[112] F. Rosquoët, A. Alexis, A. Khelidj, A. Phelipot, Experimental study of cement grout: Rheological behavior and sedimentation, Cem. Concr. Res. 33 (5) (2003) 713–722.

[113] Y. Ma, J. Hu, G. Ye, The pore structure and permeability of alkali activated fly ash, Fuel. 104 (2013) 771–780, https://doi.org/10.1016/j.fuel.2012.05.034.

[114] L. Zheng, W. Wang, Y. Shi, The effects of alkaline dosage and Si/Al ratio on the immobilization of heavy metals in municipal solid waste incineration fly ash-based geopolymer, Chemosphere. 79 (6) (2010) 665–671, https://doi.org/10.1016/j.chemosphere.2010.02.018.

[115] J. Zhang, J.L. Provis, D. Feng, J.S.J. van Deventer, Geopolymers for immobilization of Cr6+, Cd2+, and Pb2+, J. Hazard. Mater. 157 (2-3) (2008) 587–598, https://doi.org/10.1016/j.jhazmat.2008.01.053.

[116] M. Izquierdo, X. Querol, J. Davidovits, D. Antenucci, H. Nugteren, C. Fernández-Pereira, Coal fly ash-slag-based geopolymers: microstructure and metal leaching, J. Hazard. Mater. 166 (1) (2009) 561–566, https://doi.org/10.1016/j.jhazmat.2008.11.063.

[117] J.L. Provis, R.J. Myers, C.E. White, V. Rose, J.S.J. van Deventer, X-ray microtomography shows pore structure and tortuosity in alkali-activated binders, Cem. Concr. Res. 42 (6) (2012) 855–864, https://doi.org/10.1016/j.cemconres.2012.03.004.
[118] A. Fernández-Jiménez, I. Garcia-Lodeiro, O. Maltseva, A. Palomo, Mechanical-chemical activation of coal fly ashes: An effective way for recycling and make cementitious materials, Front. Mater. 6 (2019) 51.
[119] E. Adesanya, K. Ohenoja, J. Yliniemi, M. Illikainen, Mechanical transformation of phyllite mineralogy toward its use as alkali-activated binder precursor, Miner. Eng. 145 (2020), 106093, https://doi.org/10.1016/j.mineng.2019.106093.
[120] S.K. Nath, S. Kumar, Influence of granulated silico-manganese slag on compressive strength and microstructure of ambient cured alkali-activated fly ash binder, Waste Biomass Valoriz. 10 (7) (2019) 2045–2055, https://doi.org/10.1007/s12649-018-0213-1.
[121] F. Puertas, S. Martínez-Ramírez, S. Alonso, T. Vázquez, Alkali-activated fly ash/slag cements: strength behaviour and hydration products, Cem. Concr. Res. 30 (2000) 1625–1632.
[122] F.-Q. Zhao, W. Ni, H.-J. Wang, H.-J. Liu, Activated fly ash/slag blended cement, Resour. Conserv. Recycl. 52 (2) (2007) 303–313, https://doi.org/10.1016/j.resconrec.2007.04.002.
[123] N.K. Lee, H.K. Lee, Setting and mechanical properties of alkali-activated fly ash/slag concrete manufactured at room temperature, Constr. Build. Mater. 47 (2013) 1201–1209, https://doi.org/10.1016/j.conbuildmat.2013.05.107.
[124] V.S. Athira, A. Bahurudeen, M. Saljas, K. Jayachandran, Influence of different curing methods on mechanical and durability properties of alkali activated binders, Constr. Build. Mater. 299 (2021), https://doi.org/10.1016/j.conbuildmat.2021.123963.
[125] A. Abdullah, K. Hussin, M.M.A.B. Abdullah, Z. Yahya, W. Sochacki, R.A. Razak, K. Błoch, H. Fansuri, Article the effects of various concentrations of naoh on the inter-particle gelation of a fly ash geopolymer aggregate, Materials (Basel). 14 (2021) 1–11, https://doi.org/10.3390/ma14051111.
[126] M. Muraleedharan, Y. Nadir, Factors affecting the mechanical properties and microstructure of geopolymers from red mud and granite waste powder: A review, Ceram. Int. 47 (10) (2021) 13257–13279, https://doi.org/10.1016/j.ceramint.2021.02.009.
[127] R.R. Lloyd, Æ.J.L. Provis, J.S.J. Van Deventer, Microscopy and microanalysis of inorganic polymer cements . 1: remnant fly ash particles, (2009) 608–619. doi: 10.1007/s10853-008-3077-0.
[128] X. Wan, D. Hou, T. Zhao, L. Wang, Insights on molecular structure and micro-properties of alkali-activated slag materials: A reactive molecular dynamics study highlights, Constr. Build. Mater. 139 (2017) 430–437, https://doi.org/10.1016/j.conbuildmat.2017.02.049.
[129] I.I. Bashar, U.J. Alengaram, M.Z. Jumaat, A. Islam, The effect of variation of molarity of alkali activator and fine aggregate content on the compressive strength of the fly ash: Palm oil fuel ash based geopolymer mortar, Adv. Mater. Sci. Eng. 2014 (2014), https://doi.org/10.1155/2014/245473.
[130] V. Nikolić, M. Komljenović, N. Marjanović, Z. Baščarević, R. Petrović, Lead immobilization by geopolymers based on mechanically activated fly ash, Ceram. Int. 40 (6) (2014) 8479–8488, https://doi.org/10.1016/j.ceramint.2014.01.059.